# A computationally efficient 2D model for inherently equilibrated 3D stress predictions in heterogeneous laminated plates. Part I: Model formulation

R.M.J. Groh[a,*], P.M. Weaver[a]

[a] *Advanced Composites Centre for Innovation and Science, University of Bristol, Queen's Building, University Walk, Bristol, BS8 1TR, UK*

**Abstract**

Current consensus suggests a trade-off for predicting accurate 3D stress fields in multilayered plates. Relatively expensive layerwise models facilitate accurate stress predictions from underlying models assumptions, whereas more efficient equivalent single-layer theories often rely on variationally inconsistent transverse stresses from recovery steps. In contrast, we show that variationally consistent 3D stress fields are predicted from an equivalent single-layer model using a contracted form of the Hellinger-Reissner functional. Notably, this procedure facilitates computationally efficient analysis of *3D heterogeneous* plates, i.e. laminates comprising layers with material properties that differ by multiple orders of magnitude and that can also vary continuously in-plane. The model includes effects of higher-order transverse shearing and zig-zag deformations by expressing the in-plane stress field as a Taylor series expansion of global and local higher-order stress resultants. Equilibrated transverse stress assumptions are derived from Cauchy's 3D equilibrium equations, which identically satisfy the interfacial and surface traction equilibrium conditions when applied within a variational statement that enforces the 3D equilibrium equations as constraints, hence the Hellinger-Reissner mixed-variational statement. By using inherently equilibrated stress fields as model assumptions, it is shown that only the classical membrane and bending equilibrium equations have to be enforced explicitly. As a result, a contracted Hellinger-Reissner functional emerges that requires fewer displacement Lagrange multipliers than when independent stress fields are assumed. The governing equations are derived in a generalised framework such that the order of the model, and hence its accuracy, increases automatically when implemented in a computer code. By refining the order of the stress assumptions, the model is adaptable to plate-like structures ranging from thin engineering laminates to highly heterogeneous, thick laminates comprising straight-fibre or tow-steered variable-stiffness laminates, foam, honeycomb or other compliant layers.

*Keywords:* Hellinger-Reissner mixed-variational principle, Laminated variable-stiffness plates, Transverse shear deformation, Zig-zag effects

## 1. Introduction

Within the traditional applications of the aerospace and high-performance automobile industries, composite laminates are typically employed in thin-walled, semi-monocoque structures. However, with the diversification of laminated composites to primary load-bearing structures in new applications, the range of possible laminate configurations in terms of layer material properties, stacking sequences, overall laminate thicknesses, as well as the nature of service loading, is likely to expand as different applications benefit from different laminate configurations.

For example, laminated safety glass that remains intact when shattered is not only applied for ballistic protection in cars, but increasingly used as a structural material in modern office buildings. In these laminates, layers of stiff and brittle glass are joined by soft and ductile interlayers of polyvinyl butyral or ethylene-vinyl acetate [1]. As the material properties of glass and interlayer can differ by multiple orders of magnitude, the structural response to external stimuli is non-intuitive and not accurately captured using classical lamination theory. Furthermore, the use of composite laminates in regions that require thicker cross-sections, such as wind turbine blade roots, is increasing as well and these thicker aspect ratios are known to induce non-classical effects from significant transverse shearing and transverse normal deformations. In laminated composites transverse effects are exacerbated by a lack of stiff reinforcing material in the stacking direction. These transverse stresses also require particular attention as they are major drivers of common failure modes in laminated structures, such as delamination and debonding of layers.

Thus, reliable design of multilayered structures requires tools for accurate stress predictions that incorporate these non-classical effects. Currently, the standard approach in industry is to use 3D finite element models or layerwise theories to predict accurate 3D stress fields. However, these approaches are computationally prohibitive in iterative design studies as meshes with multiple elements per

*Corresponding author: rainer.groh@bristol.ac.uk

layer are typically required for converged results, and 3D layerwise models are therefore only used in areas of high stress concentration or for safety-critical components.

## 2. A discussion of the literature

In practical applications, where the thickness dimension $t$ is at least an order of magnitude smaller than representative in-plane dimensions $L_x$ and $L_y$, composite laminates are typically modelled as thin plates and shells. This feature facilitates a reduction from a 3D problem to a 2D one coincident with a chosen reference surface of the plate or shell. The major advantage of this approximation is a significant reduction in the total number of variables and computational effort required. Such a theory is aptly called an Equivalent Single-Layer Theory (ESLT) as the through-thickness properties are compressed onto a reference layer by integrating properties of interest through the thickness.

A large number of approximate, higher-order 2D theories have been formulated with the aim of predicting accurate 3D stress fields while maintaining low computational expense. Many ESLTs are based on the axiomatic approach, whereby intuitive postulations of the displacement and/or stress fields in the thickness $z$-direction are made. Appropriate displacement-based, stress-based or mixed-variational formulations are then used to derive variationally consistent governing field equations and boundary conditions.

A second possible 2D approach is the asymptotic method, whereby the 3D governing equations are expanded in terms of a small perturbation parameter $p$ and the terms related by the same power of $p^i$ grouped together. For example,

$$\mathcal{L}_{3D} \approx \mathcal{L}_1 p^1 + \mathcal{L}_2 p^2 + \cdots + \mathcal{L}_{N_o} p^{N_o} \tag{1}$$

where $\mathcal{L}_i$ is some differential operator and $N_o$ is the order of the theory. The perturbation parameter is often chosen to be the thickness to characteristic length ratio $p = t/L$, such that governing equations related to the same order of $p$ capture the significant effects at a specific length scale $(t/L)^p$. As a result, the accuracy of the solution is refined by sequentially solving the governing equations $\mathcal{L}_1$, $\mathcal{L}_2$, and so on.

The ad-hoc displacement and/or stress assumptions of axiomatic approaches facilitate an intuitive understanding of the underlying physical behaviour. For this reason, the current work focuses on axiomatic theories. The reader interested in the application of asymptotic methods to problems in structural mechanics is directed to the textbook by Ciarlet et al. [2] and a review article on the variational asymptotic method by Yu et al. [3].

### *2.1. Displacement-based theories*

The most prominent example of an axiomatic ESLT is the Classical Theory of Plates (CTP) developed by Kirchhoff [4] and then revisited by Love [5], and its extension to laminated structures, namely Classical Laminate Analysis (CLA) [6]. This theory neglects the effects of through-thickness shear and normal strains; the in-plane displacement fields $u_x$ and $u_y$ are assumed to vary linearly through the thickness; and the transverse displacement $u_z$ is assumed to be constant.

In multilayered composite structures the effects of transverse shear and normal deformations are more pronounced than for isotropic materials because the ratios of longitudinal to transverse moduli are approximately one order of magnitude greater ($E_{xx}^{iso}/G_{xz}^{iso} = 2.6$, $E_{11}/G_{13} \approx 140/5 = 28$ and $E_{xx}^{iso}/E_{zz}^{iso} = 1$, $E_{11}/E_{33} \approx 140/10 = 15$). Second, transverse anisotropy, i.e. differences in layerwise transverse shear and normal moduli, leads to sudden changes in the slopes of the three displacement fields $u_x, u_y, u_z$ at layer interfaces. This is known as the zig-zag (ZZ) phenomenon, and as shown by Demasi [7], the ZZ form of the in-plane displacements $u_x$, $u_y$ and $u_z$ can be derived directly from interfacial continuity requirements of $\tau_{xz}$, $\tau_{yz}$ and $\sigma_z$, respectively. Therefore, an accurate model for multilayered composite and sandwich structures should ideally address the modelling issues denoted as $C_z^0$-requirements by Carrera [8, 9]:

1. Through-thickness continuous displacements and transverse stresses, i.e. the interfacial continuity condition.
2. Discontinuous $z$-wise displacement derivatives at layer interfaces where transverse mechanical properties change, i.e. the ZZ effect.

At the same time, the accuracy of the model should not come at the cost of excessive computational expense if the model is to be used for iterative design studies in industry.

Refinements of the CTP along these lines have focused mainly on displacement-based models due to the relatively intuitive physical meaning of the displacement variables that govern the distortion of the plate cross-section. These theories extend from first-order shear deformation theories by Mindlin [10] and Yang, Norris and Stavsky [11] to higher-order Levinson-Reddy-type shear deformation models that enforce vanishing shear strains at the top and bottom surfaces in the displacement field *a priori* [12, 13], and further to generalised higher-order theories that do not make this initial assumption and may account for transverse normal deformation, i.e. thickness stretching [14, 15].

The body of literature on displacement-based axiomatic higher-order theories is vast and doing justice to all the different types of models in the literature is beyond the scope of this brief review. However, three general comments can be made regarding these theories. First, generalised higher-order theories are preferred over Levinson-Reddy-type models as the latter lead to static inconsistencies at clamped edges [16]. Second, an arbitrary-order theory can be conveniently expressed using the unified formulations of Carrera [9, 17, 18] and Demasi [19] by expressing the displacement field as a generalised axiomatic expansion in terms of a Taylor series or Lagrange polynomials. Third, a fundamental characteristic of purely displacement-based theories is that all strains and stresses are derived from the displacement assumptions using the kinematic and constitutive equations, respectively. Hence, the governing equations are derived using the Principle of Virtual Displacements (PVD), and once the governing equations are solved for the displacement unknowns, accurate transverse strains and transverse stresses are not recovered accurately from the kinematic relations and constitutive equations [20]. For example, the transverse shear stresses typically violate the $C_z^0$-requirements of interfacial traction continuity. More accurate transverse stresses can be recovered *a posteriori* by integrating the in-plane stresses in Cauchy's 3D indefinite equilibrium equations [21], and various techniques exist to achieve this within the displacement-based FEM [22–25]. The disadvantage of this technique is that the post-processed transverse stresses no longer satisfy the underlying equilibrium equations, and are therefore variationally inconsistent.

*2.2. Mixed-variational theories*

The aforementioned post-processing operation can be precluded if independent assumptions for the transverse stresses are made. This results in a mixed displacement/stress-based approach, whereby the governing equilibrium equations and boundary conditions are derived by means of a mixed-variational statement. For example, in the Hellinger-Reissner (HR) mixed-variational principle, the strain energy is expressed in complementary form in terms of in-plane and transverse stresses, and Cauchy's 3D equilibrium equations are introduced as constraints via Lagrange multipliers. Reissner [26, 27] was the first to use the HR principle to derive a new first-order theory for isotropic plates based on linear through-thickness assumptions of the in-plane displacement and stress fields, and inherently equilibrated quadratic transverse shear stresses.

Batra and Vidoli [28] and Batra et al. [29] used the HR principle to develop a higher-order theory for studying vibrations and plane waves in piezoelectric and anisotropic plates, accounting for both transverse shear and transverse normal deformations with all functional unknowns expanded in the thickness direction using orthonormal Legendre polynomials. The researchers showed that the major advantage of the HR principle is that by enforcing stresses to satisfy the natural boundary conditions at the top and bottom surfaces, and by deriving transverse stresses from the plate equations directly, the stress fields are closer to 3D elasticity solutions than a purely displacement-based model that relies on the constitutive equations to compute the stress fields. In particular, this means that boundary layers near clamped and free edges, and asymmetric stress profiles due to surface tractions on one surface only, can be captured more accurately.

Cosentino and Weaver [30] applied the HR principle to symmetrically laminated straight-fibre composites and derived a single sixth-order differential equation in just two variables: transverse deflection $w_0$ and bending moment function $\Omega$. The formulation of this theory is an extension of Reissner's original first-order approach for isotropic plates [26, 27] to anisotropic composite laminates. The approach by Cosentino and Weaver [30] is less general than the one proposed by Batra and Vidoli [28] as the in-plane and transverse stress assumptions are based on the same set of functional unknowns in order to minimise the computational cost. In fact, the in-plane stresses of CLA are integrated in Cauchy's equilibrium equations to derive an *a priori* equilibrated assumption for the transverse shear stresses. Recently, the present authors [31] generalised the approach by Cosentino and Weaver [30] to arbitrary-order modelling of multi-layered beams.

Another interesting contribution to the field of mixed-variational statements for composite laminates is the work by Auricchio and Sacco [32]. These authors combined a Hu-Washizu (HW) functional for the in-plane response, expressed in terms of the midplane strains and curvatures of CLA, with a HR-type functional for the transverse shear response. The transverse shear stresses were either based on independent piecewise-quadratic functions of $z$, or alternatively on equilibrated stress assumptions as in the work by Cosentino and Weaver [30]. The researchers conclude that the latter approach is the more suitable for accurate transverse shear stress results. Note that the approach by Auricchio and Sacco [32] is more computationally expensive than the model by Cosentino and Weaver [30] as the combination of HW and HR functionals in the former depends on displacement, strain and stress unknowns, whereas the pure HR functional of the latter only depends on displacements and stresses.

Forty years after publishing his work on the HR principle, Reissner [33] had the insight that when considering multilayered structures, it is sufficient to restrict the stress assumptions to the transverse stresses because only these have to be specified independently to guarantee interfacial continuity requirements. This variational statement is known as Reissner's Mixed-Variational Theory (RMVT), and makes model assumptions for the three displacements $u_x, u_y, u_z$ and independent assumptions for the transverse stresses $\tau_{xz}, \tau_{yz}, \sigma_z$. Compatibility of the transverse strains from kinematic relations, i.e. from $u_x$, $u_y$ and $u_z$, and constitutive equations, i.e. from $\tau_{xz}$, $\tau_{yz}$ and $\sigma_z$, is enforced by means of Lagrange multipliers. Hence, interfacial continuity of transverse stresses is enforced inherently via the transverse stress field assumptions, whereas the compatibility of strains is enforced variationally as a constraint condition.

Murakami [34] enhanced the axiomatic first-order displacement field assumption of Yang, Norris and Stavsky [11] by including a ZZ function, herein denoted as Murakami's ZZ function (MZZF), that alternatively takes the values of +1 or -1 at layer interfaces. Therefore, the slope purely depends on geometric differences between plies and is not based on transverse shear moduli. In addition, Murakami made independent piecewise-parabolic assumptions for the transverse shear stresses and applied RMVT to obtain new governing equations.

Recently, Gherlone [35] and the present authors [31] have shown that MZZF suffers from certain limitations for sandwiches with large face-to-core stiffness ratios and arbitrary layups, as the MZZF is not based on actual transverse shear moduli that drive the underlying physics of the problem. As an alternative ZZ function, the Refined Zigzag Theory (RZT) developed by Tessler, Di Sciuva and Gherlone [36–39] may be used. The kinematics of RZT are essentially those of a first-order shear deformation theory enhanced by ZZ variables $\psi_i(x,y)$ that are multiplied by piecewise continuous transverse functions $\phi_i^{(k)}$. Hence, in RZT,

$$u_i^{(k)}(x,y,z) = u_{0i} + z\theta_i + \phi_i^{(k)}(z)\psi_i, \quad i = x,y \tag{2a}$$

$$u_z(x,y) = w_0(x,y). \tag{2b}$$

In this theory, the ZZ slopes $\beta_x^{(k)} = \partial\phi_x^{(k)}/\partial z$ and $\beta_y^{(k)} = \partial\phi_y^{(k)}/\partial z$ for $u_x$ and $u_y$, respectively, are defined by the difference between the transverse shear rigidities $G_{xz}^{(k)}$ and $G_{yz}^{(k)}$ of layer $k$, and the effective transverse shear rigidity $G_x$ and $G_y$ of the entire layup. Thus,

$$\beta_i^{(k)} = \frac{G_i}{G_{iz}^{(k)}} - 1, \quad \text{where} \quad G_i = \left[\frac{1}{t}\sum_{k=1}^{N_l}\frac{t^{(k)}}{G_{iz}^{(k)}}\right]^{-1} \tag{3}$$

and $i = x,y$; $N_l$ is the total number of layers; and $t^{(k)}$ and $t$ are the thickness of layer $k$ and total laminate thickness, respectively. Recent work [40] suggests that the RZT ZZ function can be used to model delaminations in laminates via a cohesive damage law. The basic premise behind this approach is that the debonding process is akin to modelling a thin interfacial resin layer with heavily degraded material properties, i.e. giving rise to a ZZ deformation field.

However, the early displacement-based versions of RZT still require stress recovery steps for accurate transverse stress predictions. To remedy this deficiency, Tessler [41] recently developed a mixed-variational approach for 1D beams using RMVT in a novel way, by splitting the variation of the full RMVT functional into two separate operations. First, the variation of the Lagrange multiplier functional that enforces transverse shear strain compatibility is evaluated, and second, the variation of the strain energy functional is computed. The first step is used to derive the underlying model assumption for the transverse shear stress $\tau_{xz}$. Integrating the RZT in-plane stress $\sigma_x$ in Cauchy's axial equilibrium equation gives an expression for $\tau_{xz}$ in terms of second derivatives of the three RZT in-plane displacement variables $(u_{0x}, \theta_x, \psi_x)$ and known through-thickness functions. The second derivative terms are then replaced by ad-hoc stress functions that are determined in terms of the displacement unknowns themselves using the first variation of the Lagrange multiplier functional. Thus, the strain compatibility condition is not minimised as part of the full RMVT as was originally defined by Reissner [33]. The governing equations of the new theory, denoted by RZT$^{(m)}$, are then derived as the Euler-Lagrange equations of the strain energy functional, and are found to provide accurate transverse shear stress results from the underlying model assumption. In follow-up works the formulation was extended to plates [42, 43].

*2.3. Structure of the paper*

The aim of the present work is to develop a robust higher-order modelling framework based on a computationally efficient ESLT that predicts variationally consistent 3D stress fields in laminated beams and plates without recovering transverse stresses in post-processing steps. Particular focus is on laminated beams and plates with so-called *3D heterogeneity*, i.e. laminates comprising layers with material properties that differ by multiple orders of magnitude and that also vary continuously in the plane of the beam or plate. This latter heterogeneity arises from a new type of advanced composite known as variable-stiffness, variable angle tow or tow-steered laminate, in which the reinforcing fibres describe curvilinear paths over the planform of the plies [44–46].

The rest of the paper is structured as follows. Section 3 expresses the in-plane stress field of a plate as a generalised Taylor series expansion of the through-thickness variable $z$ multiplied by higher-order stress resultants, i.e. membrane forces and bending moments. Following the work of previous authors [30–32, 41], the in-plane stress field is then integrated in Cauchy's equilibrium equations to find expressions for the transverse shear (Section 4) and transverse normal stresses (Section 5), which inherently satisfy all interlaminar and surface traction equilibrium conditions. A new set of governing differential field equations and boundary conditions is then derived from the HR mixed-variational statement in Section 6. By using inherently equilibrated stress field assumptions it is shown that only the classical membrane and bending equilibrium equations have to be enforced in the variational statement. This results in a *contracted* HR-type functional with only two displacement Lagrange multiplier unknowns. Combined with basing all six stress fields on the same set of in-plane stress resultants, this feature considerably reduces the computational cost compared to a fully generalised HR model with independent stress field assumptions.

## 3. Higher-order zig-zag in-plane stress fields

Consider a multilayered plate of uniform thickness $t$ comprising $N_l$ perfectly bonded laminae with individual thicknesses $t^{(k)}$ as represented in Figure 1. The plies are of arbitrary linear elastic constitution and hence, may be straight-fibre or tow-steered reinforced plastic, foam, honeycomb or another compliant material. The initial configuration of the plate is referenced in orthogonal Cartesian

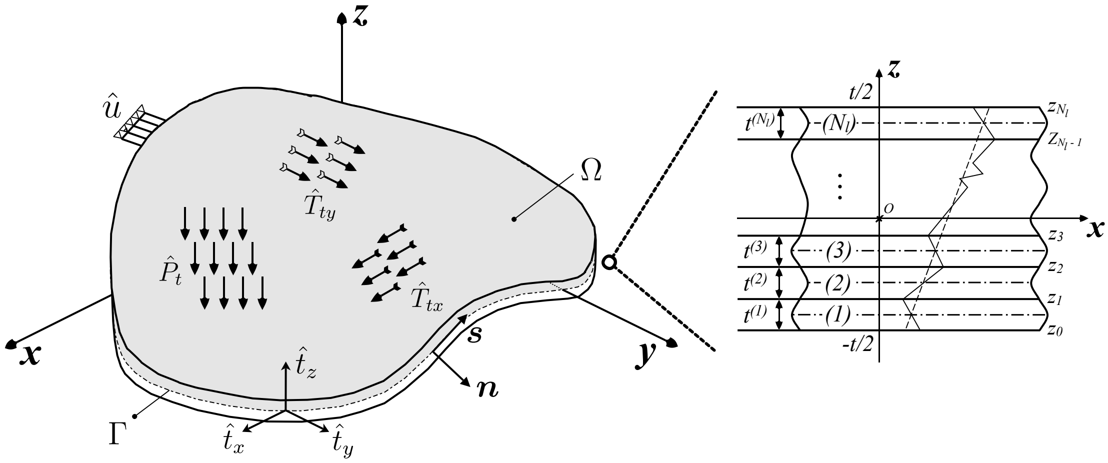

**Figure 1:** A 3D multilayered plate condensed onto an equivalent single layer. The assumed through-thickness displacement field accounts for layerwise ZZ discontinuities which are disregarded in classical theories.

coordinates $(x, y, z)$ with $x$ and $y$ defining the two in-plane dimensions and $z \in [-t/2, t/2]$ defining the thickness coordinate. In the following, this multilayered structure is condensed onto an equivalent single layer $\Omega$ coincident with the $(x, y)$-plane by integrating the structural properties and 3D governing equations in the direction of the smallest dimension $z$. The plate is bounded by two boundary surfaces $S_1$ and $S_2$ on which the displacement and traction boundary conditions are specified, respectively, and where the complete bounding surface $S = S_1 \cup S_2$. Hence, $S$ includes the top and bottom surfaces, and the circumferential boundary surface. The intersection of the bounding surface $S$ and the reference surface $\Omega$ describes the perimeter curve $\Gamma$ of the reference surface. This perimeter is split into two disjoint curves $C_1$ and $C_2$ on which displacement and stress resultant boundary conditions are prescribed, respectively. The plate is assumed to undergo static isothermal deformations under a specific set of externally applied shear and normal tractions $\left(\hat{T}_{bx}, \hat{T}_{by}, \hat{P}_b\right)$ and $\left(\hat{T}_{tx}, \hat{T}_{ty}, \hat{P}_t\right)$ on the bottom and top surfaces of the 3D body, respectively. Note that henceforth a superposed "hat" $\hat{}$ refers to a prescribed quantity, and the list $a = (a_1, a_2, a_3, \dots)$ refers to a column vector.

The in-plane displacement fields $u_x(x, y, z)$ and $u_y(x, y, z)$ are expanded as generalised expansions of $z$ in terms of global displacement variables $u_{i_n}(x, y)$ and local layerwise ZZ variables $u_i^{\phi}(x, y)$ for $i = x, y$ and $n = 0, 1, \dots, N_{o_i}$, where $N_{o_i}$ is the highest-order expansion term in the $i^{th}$ direction. We assume that practical engineering laminates maintain a high degree of transverse normal rigidity such that the present formulation ignores the occurrence of thickness stretch. Hence, $u_z(x, y)$ is independent of $z$. Therefore, only Kirchhoff's hypotheses regarding plane sections remaining plane and normals remaining perpendicular to the midplane are relaxed. Nevertheless, thickness stretch could readily be incorporated within the present formulation by assuming a higher-order global/local expansion for $u_z$ as well.

The displacement at any point $(x, y, z)$ within the plate domain is assumed to be

$$u_x^{(k)}(x, y, z) = u_{x_0}(x, y) + z u_{x_1}(x, y) + z^2 u_{x_2}(x, y) + z^3 u_{x_3}(x, y) + \dots + \phi_x^{(k)}(x, y, z) u_x^{\phi}(x, y) \tag{4a}$$

$$u_y^{(k)}(x, y, z) = u_{y_0}(x, y) + z u_{y_1}(x, y) + z^2 u_{y_2}(x, y) + z^3 u_{y_3}(x, y) + \dots + \phi_y^{(k)}(x, y, z) u_y^{\phi}(x, y) \tag{4b}$$

$$u_z(x, y) = w_0 \tag{4c}$$

where $u_{i_0}$ are in-plane displacements of the reference surface, $u_{i_1}$ are rotations of the plate cross-section, $u_{i_2}, u_{i_3}, \dots$ are higher-order stretching and rotation terms, $u_i^{\phi}$ are ZZ rotations and $\phi_i^{(k)}$ are pertinent ZZ functions where superscript $(k)$ refers to ply $k$.

Most ZZ functions in the literature can be expressed in the linear form

$$\phi_i^{(k)}(x, y, z) = m_i^{(k)}(x, y) \cdot z + c_i^{(k)}(x, y) \quad \text{for} \quad i = x, y \tag{5}$$

where $m_i^{(k)}$ and $c_i^{(k)}$ take different layerwise values depending on the particular choice of the ZZ function. The RZT ZZ function $\phi_{RZT}^{(k)}$ in two dimensions, introduced by Tessler et al. [37], is defined by

$$\left.\begin{aligned}\phi^{(1)}_{i_{RZT}}(x,y,z) &= \left(z+\frac{t}{2}\right)\left(\frac{G_i(x,y)}{G^{(1)}_{iz}(x,y)}-1\right)\\ \phi^{(k)}_{i_{RZT}}(x,y,z) &= \left(z+\frac{t}{2}\right)\left(\frac{G_i(x,y)}{G^{(k)}_{iz}(x,y)}-1\right)+\sum_{j=2}^{k} t^{(j-1)}\left(\frac{G_i(x,y)}{G^{(j-1)}_{iz}(x,y)}-\frac{G_i(x,y)}{G^{(k)}_{iz}(x,y)}\right)\end{aligned}\right\} \text{for } i=x,y \tag{6}$$

$$\text{and } G_i(x,y)=\left[\frac{1}{t}\sum_{k=1}^{N_l}\frac{t^{(k)}}{G^{(k)}_{iz}(x,y)}\right]^{-1}.$$

For for advanced composites with curvilinear fibre paths, the RZT ZZ function is not only a layerwise quantity, but also varies with the in-plane coordinates $(x, y)$ as the transverse shear moduli $G^{(k)}_{iz}(x, y)$ can change from point to point over surface $\Omega$.

MZZF, on the other hand, is invariant of transverse material properties and therefore only varies with location $(x, y)$ when the thickness of the plate changes. In the case of a constant thickness plate, MZZF is purely a layerwise function given by

$$\phi^{(k)}_{i_{MZZF}}(z) = (-1)^k \frac{2}{t^{(k)}}\left(z - z^{(k)}_m\right) \quad \text{for} \quad i = x, y \tag{7}$$

where $z^{(k)}_m$ is the midplane coordinate of layer $k$. Note that for a constant thickness plate $\phi^{(k)}_{x_{MZZF}} = \phi^{(k)}_{y_{MZZF}}$.

To facilitate the concise derivation of the governing equations, the displacement field Eq. (4) is expressed in condensed matrix form as follows:

$$\mathcal{U}^{(k)}_{xy} = \begin{Bmatrix} u^{(k)}_x \\ u^{(k)}_y \end{Bmatrix} = \begin{bmatrix}\boldsymbol{I}_2 & \boldsymbol{Z}_2 & \boldsymbol{Z}_2^2 & \ldots\end{bmatrix}\begin{Bmatrix}\mathcal{U}^g_0\\ \mathcal{U}^g_1 \\ \mathcal{U}^g_2 \\ \vdots\end{Bmatrix} + \begin{bmatrix}\phi^{(k)}_x & 0 \\ 0 & \phi^{(k)}_y\end{bmatrix}\begin{Bmatrix}u^\phi_x \\ u^\phi_y\end{Bmatrix} \tag{8}$$

where the matrices and vectors in Eq. (8) are given by

$$\boldsymbol{I}_2 = \begin{bmatrix}1 & 0\\ 0 & 1\end{bmatrix},\ \boldsymbol{Z}_2 = \begin{bmatrix}z & 0\\ 0 & z\end{bmatrix},\ \boldsymbol{Z}_2^2 = \begin{bmatrix}z^2 & 0\\ 0 & z^2\end{bmatrix},\ \ldots \tag{9}$$

$$\mathcal{U}^g_0 = \left[u_{x_0}\ u_{y_0}\right]^\top,\ \mathcal{U}^g_1 = \left[u_{x_1}\ u_{y_1}\right]^\top,\ \mathcal{U}^g_2 = \left[u_{x_2}\ u_{y_2}\right]^\top,\ \ldots \tag{10}$$

with superscript $g$ henceforth defined to refer to global quantities, and $\top$ to denote the matrix transpose. By defining,

$$\boldsymbol{f}^g_u = \begin{bmatrix}\boldsymbol{I}_2 & \boldsymbol{Z}_2 & \boldsymbol{Z}_2^2 & \ldots\end{bmatrix} \text{ and } \boldsymbol{f}^l_u = \begin{bmatrix}\phi^{(k)}_x & 0\\ 0 & \phi^{(k)}_y\end{bmatrix}, \tag{11}$$

$$\mathcal{U}^g = \begin{bmatrix}\mathcal{U}^g_0 & \mathcal{U}^g_1 & \mathcal{U}^g_2 & \ldots\end{bmatrix}^\top \text{ and } \mathcal{U}^l = \begin{bmatrix}u^\phi_x & u^\phi_y\end{bmatrix}^\top \tag{12}$$

where superscript $l$ is henceforth defined to refer to local ZZ quantities, Eq. (8) now reads

$$\mathcal{U}^{(k)}_{xy} = \boldsymbol{f}^g_u\mathcal{U}^g + \boldsymbol{f}^l_u\mathcal{U}^l = \begin{bmatrix}\boldsymbol{f}^g_u & \boldsymbol{f}^l_u\end{bmatrix}\begin{Bmatrix}\mathcal{U}^g\\ \mathcal{U}^l\end{Bmatrix} = \boldsymbol{f}^{(k)}_u\mathcal{U} \tag{13}$$

The in-plane strains $\epsilon$ in Voigt-Kelvin vector notation are now derived from the kinematic relations,

$$\epsilon = \begin{Bmatrix}\epsilon_x\\ \epsilon_y\\ \gamma_{xy}\end{Bmatrix} = \begin{Bmatrix}\dfrac{\partial u_x}{\partial x}\\ \dfrac{\partial u_y}{\partial y}\\ \dfrac{\partial u_x}{\partial y}+\dfrac{\partial u_y}{\partial x}\end{Bmatrix} = \begin{bmatrix}\dfrac{\partial}{\partial x} & 0\\ 0 & \dfrac{\partial}{\partial y}\\ \dfrac{\partial}{\partial y} & \dfrac{\partial}{\partial x}\end{bmatrix}\begin{Bmatrix}u_x\\ u_y\end{Bmatrix} = \boldsymbol{D}\mathcal{U}_{xy} \tag{14}$$

where a new differential operator matrix $\boldsymbol{D}$ has been defined. Substituting the expression for $\mathcal{U}_{xy}$ from Eq. (13) into the kinematic relations Eq. (14) gives

$$\begin{aligned}\epsilon^{(k)} = {} & \begin{bmatrix}\boldsymbol{I}_3 & \boldsymbol{Z}_3 & \boldsymbol{Z}_3^2 & \ldots\end{bmatrix}\begin{bmatrix}\boldsymbol{D} & 0 & 0 & \ldots\\ 0 & \boldsymbol{D} & 0 & \ldots\\ 0 & 0 & \boldsymbol{D} & \ldots\\ \vdots & \vdots & \vdots & \ddots\end{bmatrix}\begin{Bmatrix}\mathcal{U}^g_0\\ \mathcal{U}^g_1\\ \mathcal{U}^g_2\\ \vdots\end{Bmatrix} + \\ & \begin{bmatrix}\phi^{(k)}_x & 0 & 0 & 0\\ 0 & \phi^{(k)}_y & 0 & 0\\ 0 & 0 & \phi^{(k)}_x & \phi^{(k)}_y\end{bmatrix}\begin{bmatrix}\dfrac{\partial}{\partial x} & 0\\ 0 & \dfrac{\partial}{\partial y}\\ \dfrac{\partial}{\partial y} & 0\\ 0 & \dfrac{\partial}{\partial x}\end{bmatrix}\begin{Bmatrix}u^\phi_x\\ u^\phi_y\end{Bmatrix} + \\ & \left(\begin{bmatrix}\dfrac{\partial}{\partial x} & 0\\ 0 & \dfrac{\partial}{\partial y}\\ \dfrac{\partial}{\partial y} & \dfrac{\partial}{\partial x}\end{bmatrix}\begin{bmatrix}\phi^{(k)}_x & 0\\ 0 & \phi^{(k)}_y\end{bmatrix}\right)\begin{Bmatrix}u^\phi_x\\ u^\phi_y\end{Bmatrix}\end{aligned} \tag{15}$$

where $\boldsymbol{I}_3$, $\boldsymbol{Z}_3$, $\boldsymbol{Z}_3^2$ etc. are 3x3 versions of the 2x2 matrices defined in Eq. (9), and the differential operator matrix in the third term of Eq. (15) is only applied on the ZZ function matrix within the parentheses. Note that this particular term in parentheses vanishes when MZZF is used. By defining the following $z$-wise expansion functions

$$\boldsymbol{f}^g_\epsilon = \begin{bmatrix}\boldsymbol{I}_3 & \boldsymbol{Z}_3 & \boldsymbol{Z}_3^2 & \dots\end{bmatrix}$$
$$\boldsymbol{f}^l_\epsilon = \begin{bmatrix}\phi_x^{(k)} & 0 & 0 & 0\\ 0 & \phi_y^{(k)} & 0 & 0\\ 0 & 0 & \phi_x^{(k)} & \phi_y^{(k)}\end{bmatrix} \tag{16}$$

and differential operator matrices

$$\boldsymbol{D}^g = \begin{bmatrix}\boldsymbol{D} & 0 & 0 & \dots\\ 0 & \boldsymbol{D} & 0 & \dots\\ 0 & 0 & \boldsymbol{D} & \dots\\ \vdots & \vdots & \vdots & \ddots\end{bmatrix} \quad \text{and } \boldsymbol{D}^l = \begin{bmatrix}\dfrac{\partial}{\partial x} & 0\\ 0 & \dfrac{\partial}{\partial y}\\ \dfrac{\partial}{\partial y} & 0\\ 0 & \dfrac{\partial}{\partial x}\end{bmatrix} \tag{17}$$

the in-plane strain Eq. (15) is simplified to

$$\epsilon^{(k)} = \boldsymbol{f}^g_\epsilon \left(\boldsymbol{D}^g \mathcal{U}^g\right) + \boldsymbol{f}^l_\epsilon \left(\boldsymbol{D}^l \mathcal{U}^l\right) + \left(\boldsymbol{D}\boldsymbol{f}^l_u\right)\mathcal{U}^l. \tag{18}$$

Finally, by defining the global and local strain fields $\epsilon^g$ and $\epsilon^l$, respectively,

$$\epsilon^g = \boldsymbol{D}^g \mathcal{U}^g \quad \text{and} \quad \epsilon^l = \boldsymbol{D}^l \mathcal{U}^l \tag{19}$$

the strain can simply be expressed as

$$\epsilon^{(k)} = \begin{bmatrix}\boldsymbol{f}^g_\epsilon & \boldsymbol{f}^l_\epsilon & \boldsymbol{D}\boldsymbol{f}^l_u\end{bmatrix}\begin{Bmatrix}\epsilon^g\\ \epsilon^l\\ \mathcal{U}^l\end{Bmatrix} = \boldsymbol{f}^{(k)}_\epsilon \mathcal{E}. \tag{20}$$

As a result, the in-plane strains are now defined as a product of a through-thickness function $\boldsymbol{f}^{(k)}_\epsilon$ and unknown field variables $\mathcal{E}$. Note that when MZZF is used $\boldsymbol{D}\boldsymbol{f}^l_u = \boldsymbol{0}$ and therefore the variables $\mathcal{U}^l$ in $\mathcal{E}$ are eliminated.

The in-plane stresses $\sigma$, expressed in Voigt-Kelvin vector notation are now calculated from the strains using the reduced stiffness matrix $\bar{\boldsymbol{Q}}$ for plane stress in $z$. Hence,

$$\begin{aligned}\sigma^{(k)} = \begin{Bmatrix}\sigma_x\\ \sigma_y\\ \sigma_{xy}\end{Bmatrix}^{(k)} &= \begin{bmatrix}\bar{Q}_{11} & \bar{Q}_{12} & \bar{Q}_{16}\\ \bar{Q}_{12} & \bar{Q}_{22} & \bar{Q}_{26}\\ \bar{Q}_{16} & \bar{Q}_{26} & \bar{Q}_{66}\end{bmatrix}^{(k)} \begin{Bmatrix}\epsilon_x\\ \epsilon_y\\ \gamma_{xy}\end{Bmatrix}^{(k)}\\ &= \bar{\boldsymbol{Q}}^{(k)}\epsilon^{(k)} = \bar{\boldsymbol{Q}}^{(k)}\boldsymbol{f}^{(k)}_\epsilon \mathcal{E}.\end{aligned} \tag{21}$$

The stress resultants $\mathcal{F}$ are defined as the through-thickness integrals of the in-plane stresses $\sigma^{(k)}$ multiplied by the assumed strain field function $\boldsymbol{f}^{(k)}_\epsilon$. As the in-plane stress dyad $\boldsymbol{\sigma} = \sigma_{ij},\ i,j = x,y$ has been expressed as a vector in Voigt-Kelvin notation, i.e. $\sigma^{(k)} = (\sigma_x, \sigma_y, \sigma_{xy})$, $\mathcal{F}$ is a collection of stress resultants expressed in Voigt-Kelvin notation as well. Thus,

$$\begin{aligned}\mathcal{F} = \int_{-t/2}^{t/2} \boldsymbol{f}^{(k)^\top}_\epsilon \sigma^{(k)} \mathrm{d}z &= \int_{-t/2}^{t/2} \boldsymbol{f}^{(k)^\top}_\epsilon \bar{\boldsymbol{Q}}^{(k)} \boldsymbol{f}^{(k)}_\epsilon \mathrm{d}z \cdot \mathcal{E}\\ &= \boldsymbol{S}\cdot\mathcal{E}\end{aligned} \tag{22}$$

where the first six terms of the column vector $\mathcal{F} = (N_x, N_y, N_{xy}, M_x, M_y, M_{xy}, \dots)$ are the classical membrane forces and bending moments $\mathcal{N} = (N_x, N_y, N_{xy})$ and $\mathcal{M} = (M_x, M_y, M_{xy})$, and the following terms in $\mathcal{F}$ are higher-order moments.

In general, the orders of expansion in the $x$- and $y$-directions are chosen to be the same such that $N_{o_x} = N_{o_y} = N_o$. In this case, the length $\mathcal{O}$ of the stress resultant vector $\mathcal{F}$ is given by:

- Global expansion up to $z^{N_o}$, no ZZ variables: $\mathcal{O} = 3(N_o + 1)$
- Global expansion up to $z^{N_o}$, MZZF: $\mathcal{O} = 3(N_o+1) + 3$
- Global expansion up to $z^{N_o}$, RZT: $\mathcal{O} = 3(N_o+1) + 6$. Note, $\mathcal{O} = 3(N_o+1) + 4$ for straight-fibre laminates.

Thus, a model based on RZT can lead up to three more variables in $\mathcal{F}$ than a model based on MZZF. In the general case of RZT $\phi_x^{(k)} \neq \phi_y^{(k)}$, and therefore the ZZ twisting moments

$$M^\phi_{xy} = \int_{-t/2}^{t/2} \phi_x^{(k)}\sigma_{xy}^{(k)}\mathrm{d}z \quad \neq \quad M^\phi_{yx} = \int_{-t/2}^{t/2} \phi_y^{(k)}\sigma_{xy}^{(k)}\mathrm{d}z, \tag{23}$$

whereas for MZZF $M^\phi_{xy} = M^\phi_{yx}$. Second, in the general case of varying material properties over the planform, e.g. for tow-steered laminates, the RZT coefficient matrix $\boldsymbol{D}\boldsymbol{f}^l_u \neq \boldsymbol{0}$, which leads to two extra moments associated with the derivatives of the ZZ function. Hence,

$$\begin{aligned}M^{\partial\phi}_x &= \int_{-t/2}^{t/2} \left(\frac{\partial\phi_x^{(k)}}{\partial x}\sigma_x + \frac{\partial\phi_x^{(k)}}{\partial y}\sigma_{xy}\right)\mathrm{d}z\\ M^{\partial\phi}_y &= \int_{-t/2}^{t/2} \left(\frac{\partial\phi_y^{(k)}}{\partial y}\sigma_y + \frac{\partial\phi_y^{(k)}}{\partial x}\sigma_{xy}\right)\mathrm{d}z\end{aligned} \tag{24}$$

and therefore, combined with the fact that $M^\phi_{xy} \neq M^\phi_{yx}$, RZT defines three more stress resultants than MZZF.

Finally, matrix $\boldsymbol{S}$ in Eq. (22) is the higher-order ABD stiffness matrix of dimensions $\mathcal{O}\times\mathcal{O}$ defined by

$$\boldsymbol{S} = \int_{-t/2}^{t/2} \boldsymbol{f}^{(k)^\top}_\epsilon \bar{\boldsymbol{Q}}^{(k)} \boldsymbol{f}^{(k)}_\epsilon \mathrm{d}z \tag{25}$$

which can be inverted to express the unknown strain field $\mathcal{E}$ in Eq. (22) in terms of the stress resultants $\mathcal{F}$. Hence,

$$\mathcal{E} = \boldsymbol{S}^{-1}\mathcal{F} = \boldsymbol{s}\mathcal{F} \quad \text{where} \quad \boldsymbol{s} = \boldsymbol{S}^{-1}. \tag{26}$$

Thus, we have derived a general expression for the layerwise in-plane stresses $\sigma^{(k)}$ given by

$$\sigma^{(k)} = \bar{\boldsymbol{Q}}^{(k)}\boldsymbol{f}^{(k)}_\epsilon \boldsymbol{s}\mathcal{F} \tag{27}$$

in terms of layerwise constitutive matrices $\bar{\boldsymbol{Q}}^{(k)}$, the higher-order compliance matrix $\boldsymbol{s}$, through-thickness shape functions $\boldsymbol{f}_\epsilon^{(k)}$ and the stress resultants $\mathcal{F}$, where the latter are the only functional unknowns.

Note, the advantage of expressing the in-plane stresses in terms of stress resultants rather than displacements is that the stresses are now functions of the unknown variables themselves rather than their derivatives, and this helps to reduce the order of the derived differential equations. In general, lower-order differential equations can be solved with less numerical discretisation error.

## 4. Derivation of transverse shear stress fields

An expression for the transverse shear stresses is found by integrating the axial stresses of Eq. (27) in Cauchy's in-plane equilibrium equations in the absence of body forces,

$$\begin{aligned}\frac{\partial \sigma_{xz}^{(k)}}{\partial z} &= -\frac{\partial \sigma_{x}^{(k)}}{\partial x} - \frac{\partial \sigma_{xy}^{(k)}}{\partial y}\\ \frac{\partial \sigma_{yz}^{(k)}}{\partial z} &= -\frac{\partial \sigma_{xy}^{(k)}}{\partial x} - \frac{\partial \sigma_{y}^{(k)}}{\partial y}\end{aligned} \tag{28}$$

and therefore

$$\begin{aligned}\frac{\partial \tau^{(k)}}{\partial z} &= \frac{\partial}{\partial z}\begin{Bmatrix}\sigma_{xz}\\ \sigma_{yz}\end{Bmatrix}^{(k)} = -\begin{bmatrix}\frac{\partial}{\partial x} & 0 & \frac{\partial}{\partial y}\\ 0 & \frac{\partial}{\partial y} & \frac{\partial}{\partial x}\end{bmatrix}\begin{Bmatrix}\sigma_x\\ \sigma_y\\ \sigma_{xy}\end{Bmatrix}^{(k)}\\ &= -\boldsymbol{D}^\top \sigma^{(k)} = -\boldsymbol{D}^\top\left[\bar{\boldsymbol{Q}}^{(k)}\boldsymbol{f}_\epsilon^{(k)}\boldsymbol{s}\mathcal{F}\right].\end{aligned} \tag{29}$$

Note, the differential operator matrix $\boldsymbol{D}^\top$ is applied to all terms within the square brackets as both the material dependent quantities $\bar{\boldsymbol{Q}}^{(k)}$, $\boldsymbol{f}_\epsilon^{(k)}$ and $\boldsymbol{s}$, as well as the stress resultants $\mathcal{F}$ can vary over the domain $\Omega$ of a plate with curvilinear fibres. The only term in Eq. (29) that is a function of $z$ is $\boldsymbol{f}_\epsilon^{(k)}$ and therefore only this term is integrated to derive the transverse shear stresses. Hence,

$$\begin{aligned}\tau^{(k)} &= -\boldsymbol{D}^\top\left[\bar{\boldsymbol{Q}}^{(k)}\left(\int \boldsymbol{f}_\epsilon^{(k)}(z)\mathrm{d}z\right)\boldsymbol{s}\mathcal{F}\right]\\ &= -\boldsymbol{D}^\top\left[\bar{\boldsymbol{Q}}^{(k)}\boldsymbol{g}^{(k)}(z)\boldsymbol{s}\mathcal{F}\right] + \boldsymbol{a}^{(k)}\end{aligned} \tag{30}$$

where $\boldsymbol{g}^{(k)}(z)$ captures the variation of $\tau^{(k)}$ through the thickness of each ply $k$ and is derived by simple integration of the local and global polynomial shape functions.

The $N_l$ layerwise constants $\boldsymbol{a}^{(k)}$ are found by enforcing the $N_l - 1$ interfacial continuity conditions $\tau^{(k)}(z_{k-1}) = \tau^{(k-1)}(z_{k-1})$ for $k = 2, \ldots, N_l$, and one of the prescribed surface tractions, i.e. either the bottom surface $\tau^{(1)}(z_0) = \hat{T}_b = \begin{bmatrix}\hat{T}_{bx} & \hat{T}_{by}\end{bmatrix}^\top$ or the top surface $\tau^{(N_l)}(z_{N_l}) = \hat{T}_t = \begin{bmatrix}\hat{T}_{tx} & \hat{T}_{ty}\end{bmatrix}^\top$ tractions. Here, we choose to enforce the bottom surface tractions such that the layerwise constants are found to be

$$\begin{aligned}\boldsymbol{a}^{(k)} &= \sum_{i=1}^{k}\boldsymbol{D}^\top\Big[\Big\{\bar{\boldsymbol{Q}}^{(i)}\boldsymbol{g}^{(i)}(z_{i-1}) - \\ &\qquad \bar{\boldsymbol{Q}}^{(i-1)}\boldsymbol{g}^{(i-1)}(z_{i-1})\Big\}\boldsymbol{s}\mathcal{F}\Big] + \hat{T}_b\\ \boldsymbol{a}^{(k)} &= \boldsymbol{D}^\top\left[\boldsymbol{\alpha}^{(k)}\boldsymbol{s}\mathcal{F}\right] + \hat{T}_b\end{aligned} \tag{31}$$

where by definition $\bar{\boldsymbol{Q}}^0 = \boldsymbol{0}$ and the variable

$$\boldsymbol{\alpha}^{(k)} = \sum_{i=1}^{k}\left\{\bar{\boldsymbol{Q}}^{(i)}\boldsymbol{g}^{(i)}(z_{i-1}) - \bar{\boldsymbol{Q}}^{(i-1)}\boldsymbol{g}^{(i-1)}(z_{i-1})\right\} \tag{32}$$

has been introduced. Additional physical insight into the layerwise integration constants $\boldsymbol{\alpha}^{(k)}$ can be gleaned when considering that the higher-order ABD matrix defined in Eq. (25) is equal to the through-thickness integral of layerwise constitutive matrices $\bar{\boldsymbol{Q}}^{(k)}$ multiplied by shape functions $\boldsymbol{f}_\epsilon^{(k)}$. As $\boldsymbol{g}^{(k)}$ is equal to the indefinite integral of $\boldsymbol{f}_\epsilon^{(k)}$, the $\boldsymbol{\alpha}^{(k)}$ terms can be interpreted as the partial higher-order ABD matrices up to the $k^{th}$ layer.

The final expression for $\tau^{(k)}$ is established by substituting the layerwise integration constants of Eq. (31) back into Eq. (30). Thus,

$$\tau^{(k)} = \boldsymbol{D}^\top\left[\left(-\bar{\boldsymbol{Q}}^{(k)}\boldsymbol{g}^{(k)}(z) + \boldsymbol{\alpha}^{(k)}\right)\boldsymbol{s}\mathcal{F}\right] + \hat{T}_b. \tag{33}$$

In the derivation of Eq. (31), the surface traction on the top surface is not enforced explicitly. As the proof below shows, this condition is automatically satisfied if equilibrium of the axial stress field Eq. (27) and transverse shear stress Eq. (33) is enforced. As we are dealing with an equivalent single layer, Cauchy's two in-plane equilibrium equations in the absence of body forces are integrated in the thickness $z$-direction to give

$$\int_{-t/2}^{t/2}\left(\boldsymbol{D}^\top\sigma^{(k)} + \frac{\partial \tau^{(k)}}{\partial z}\right)\mathrm{d}z = \boldsymbol{D}^\top\mathcal{N} + \hat{T}_t - \hat{T}_b = \boldsymbol{0} \tag{34}$$

where the column vector $\mathcal{N} = (N_x, N_y, N_{xy})$ represents the membrane stress resultants, and the substitutions $\hat{T}_t = \tau^{(N_l)}(z_{N_l})$ and $\hat{T}_b = \tau^{(1)}(z_0)$ have been made. An expression for $\boldsymbol{D}^\top\mathcal{N}$ is readily derived by applying the differential operator matrix $\boldsymbol{D}^\top$ to the expression for $\sigma^{(k)}$ in Eq. (27) and then integrating in the $z$-direction. Hence,

$$\begin{aligned}\boldsymbol{D}^\top\mathcal{N} &= \int_{-t/2}^{t/2}\boldsymbol{D}^\top\sigma^{(k)}\mathrm{d}z\\ &= \sum_{k=1}^{N_l}\boldsymbol{D}^\top\left[\left\{\bar{\boldsymbol{Q}}^{(k)}\boldsymbol{g}^{(k)}(z_k) - \bar{\boldsymbol{Q}}^{(k)}\boldsymbol{g}^{(k)}(z_{k-1})\right\}\boldsymbol{s}\mathcal{F}\right].\end{aligned} \tag{35}$$

Next, an expression for $\hat{T}_t$, which was the only traction not enforced explicitly in the computation of the integration constants of Eq. (31), is sought using the expression for $\tau^{(k)}$ in Eq. (33),

$$\tau^{(N_l)}(z_{N_l}) = \boldsymbol{D}^\top \left[\left\{-\bar{\boldsymbol{Q}}^{(N_l)}\boldsymbol{g}^{(N_l)}(z_{N_l}) + \boldsymbol{\alpha}^{(N_l)}\right\}\boldsymbol{s}\mathcal{F}\right] + \hat{T}_b$$

$$\hat{T}_t = -\sum_{k=1}^{N_l} \boldsymbol{D}^\top \left[\left\{\bar{\boldsymbol{Q}}^{(k)}\boldsymbol{g}^{(k)}(z_k) - \bar{\boldsymbol{Q}}^{(k)}\boldsymbol{g}^{(k)}(z_{k-1})\right\}\boldsymbol{s}\mathcal{F}\right] + \hat{T}_b. \quad (36)$$

Substituting Eq. (35) into Eq. (36) we have

$$\hat{T}_t = -\boldsymbol{D}^\top\mathcal{N} + \hat{T}_b \quad (37)$$

and by substituting Eq. (37) back into Cauchy's equilibrium Eq. (34) gives

$$\boldsymbol{D}^\top\mathcal{N} + \left(-\boldsymbol{D}^\top\mathcal{N} + \hat{T}_b\right) - \hat{T}_b = \boldsymbol{0}. \quad (38)$$

Hence, the expression in Eq. (38) is satisfied identically. This is the first important characteristic of the higher-order model presented herein; as long as Cauchy's in-plane equilibrium equations (34) are enforced when deriving the governing equations from a variational statement, equilibrium of the interfacial and surface shear tractions is automatically guaranteed *a priori* using the stress assumptions in Eqs. (27) and (33).

Finally, the layerwise coefficients in the expression for $\tau^{(k)}$ in Eq. (33), namely $-\bar{\boldsymbol{Q}}^{(k)}\boldsymbol{g}^{(k)} + \boldsymbol{\alpha}^{(k)}$ are conveniently combined into a single layerwise array $\boldsymbol{c}^{(k)}(z)$ such that

$$\tau^{(k)} = \boldsymbol{D}^\top \left[\boldsymbol{c}^{(k)}\boldsymbol{s}\mathcal{F}\right] + \hat{T}_b. \quad (39)$$

To shed some further insight into the transverse shear stresses in Eq. (39), the term $\boldsymbol{R}^{(k)} = \boldsymbol{c}^{(k)}\boldsymbol{s}$ is defined and the differential product rule applied to expand the term

$$\begin{aligned}\boldsymbol{D}^\top\left(\boldsymbol{c}^{(k)}\boldsymbol{s}\mathcal{F}\right) &= \boldsymbol{D}^\top\left(\boldsymbol{R}^{(k)}\mathcal{F}\right)\\ &= \left(\boldsymbol{D}^\top\boldsymbol{R}^{(k)}\right)\mathcal{F} + \boldsymbol{I}_x\boldsymbol{R}^{(k)}\frac{\partial\mathcal{F}}{\partial x} + \boldsymbol{I}_y\boldsymbol{R}^{(k)}\frac{\partial\mathcal{F}}{\partial y}\\ &= \left(\boldsymbol{D}^\top\boldsymbol{R}^{(k)}\right)\mathcal{F} + \boldsymbol{R}_x^{(k)}\frac{\partial\mathcal{F}}{\partial x} + \boldsymbol{R}_y^{(k)}\frac{\partial\mathcal{F}}{\partial y}\end{aligned} \quad (40)$$

where the parentheses in the first term indicate that the differential operator matrix $\boldsymbol{D}^\top$ is only applied to matrix $\boldsymbol{R}^{(k)}$, and the matrices

$$\boldsymbol{I}_x = \begin{bmatrix}1 & 0 & 0\\ 0 & 0 & 1\end{bmatrix} \text{ and } \boldsymbol{I}_y = \begin{bmatrix}0 & 0 & 1\\ 0 & 1 & 0\end{bmatrix} \quad (41)$$

have been introduced to allow the partial derivatives $\partial/\partial x$ and $\partial/\partial y$ to be applied directly to $\mathcal{F}$ with coefficients of $\boldsymbol{R}_x^{(k)} = \boldsymbol{I}_x\boldsymbol{R}^{(k)}$ and $\boldsymbol{R}_y^{(k)} = \boldsymbol{I}_y\boldsymbol{R}^{(k)}$. By substituting Eq. (40) into Eq. (39), an alternative definition of $\tau^{(k)}$ in terms of the layerwise constitutive matrices $\boldsymbol{R}^{(k)}$, $\boldsymbol{R}_x^{(k)}$ and $\boldsymbol{R}_y^{(k)}$ is derived,

$$\tau^{(k)} = \left(\boldsymbol{D}^\top\boldsymbol{R}^{(k)}\right)\mathcal{F} + \boldsymbol{R}_x^{(k)}\frac{\partial\mathcal{F}}{\partial x} + \boldsymbol{R}_y^{(k)}\frac{\partial\mathcal{F}}{\partial y} + \hat{T}_b. \quad (42)$$

The significance of Eq. (42) is two-fold. First, separating the derivatives of $\mathcal{F}$ allows for straightforward manipulations of the integration-by-parts step involved in the derivation of the Euler-Lagrange equations via the calculus of variations in Section 6. Second, the first term $\boldsymbol{D}^\top\boldsymbol{R}^{(k)}$ in Eq. (42) is only non-zero for variable-stiffness laminates as it includes derivatives of material properties $\boldsymbol{R}^{(k)}$. Thus, Eq. (42) decomposes the contributions of the transverse shear stresses into the linear superposition of variable-stiffness and constant-stiffness components.

## 5. Derivation of transverse normal stress field

An expression for the transverse normal stress is derived in a similar fashion by integrating Cauchy's transverse equilibrium equation in the absence of body forces. Thus,

$$\frac{\partial\sigma_z^{(k)}}{\partial z} = -\begin{bmatrix}\frac{\partial}{\partial x} & \frac{\partial}{\partial y}\end{bmatrix}\begin{Bmatrix}\sigma_{xz}^{(k)}\\ \sigma_{yz}^{(k)}\end{Bmatrix} = -\nabla^\top\tau^{(k)}$$

where $\nabla = \left(\frac{\partial}{\partial x}, \frac{\partial}{\partial y}\right)$ is the del operator used to calculate the divergence of $\tau^{(k)}$. Subsituting for $\tau^{(k)}$ using Eq. (33) and integrating in the $z$-direction,

$$\begin{aligned}\sigma_z^{(k)} &= \nabla^\top\boldsymbol{D}^\top\left[\int\left(\bar{\boldsymbol{Q}}^{(k)}\boldsymbol{g}^{(k)}(z) - \boldsymbol{\alpha}^{(k)}\right)\mathrm{d}z\boldsymbol{s}\mathcal{F}\right] - \nabla^\top\hat{T}_b z\\ &= \nabla^\top\boldsymbol{D}^\top\left[\left\{\bar{\boldsymbol{Q}}^{(k)}\boldsymbol{h}^{(k)}(z) - \boldsymbol{\alpha}^{(k)}z\right\}\boldsymbol{s}\mathcal{F}\right] - \nabla^\top\hat{T}_b z + \boldsymbol{b}^{(k)}\end{aligned} \quad (43)$$

where $\boldsymbol{h}^{(k)}(z)$ captures the variation of $\sigma_z^{(k)}$ through the thickness of each ply $k$ and is readily derived by integrating the assumed polynomial shape functions.

The $N_l$ layerwise constants $\boldsymbol{b}^{(k)}$ are found by enforcing the $N_l - 1$ continuity conditions $\sigma_z^{(k)}(z_{k-1}) = \sigma_z^{(k-1)}(z_{k-1})$ for $k = 2, \ldots, N_l$, and one of the prescribed surface tractions, i.e. either the bottom surface $\sigma_z^{(1)}(z_0) = \hat{P}_b$ or the top surface $\sigma_z^{(N_l)}(z_{N_l}) = \hat{P}_t$ traction. Here, we choose to enforce the bottom traction condition such that the integration constants are

$$\begin{aligned}\boldsymbol{b}^{(k)} &= \nabla^\top\boldsymbol{D}^\top\sum_{i=1}^{k}\left[\left\{\bar{\boldsymbol{Q}}^{(i-1)}\boldsymbol{h}^{(i-1)}(z_{i-1}) - \bar{\boldsymbol{Q}}^{(i)}\boldsymbol{h}^{(i)}(z_{i-1}) + \left(\boldsymbol{\alpha}^{(i)} - \boldsymbol{\alpha}^{(i-1)}\right)z_{i-1}\right\}\boldsymbol{s}\mathcal{F}\right] + \nabla^\top\hat{T}_b z_0 + \hat{P}_b\\ &= \nabla^\top\boldsymbol{D}^\top\left[\boldsymbol{\beta}^{(k)}\boldsymbol{s}\mathcal{F}\right] + \nabla^\top\hat{T}_b z_0 + \hat{P}_b\end{aligned} \quad (44)$$

where by definition $\bar{\boldsymbol{Q}}^0 = \boldsymbol{\alpha}^0 = \boldsymbol{0}$ and the variable $\boldsymbol{\beta}^{(k)}$ has been introduced,

$$\boldsymbol{\beta}^{(k)} = \sum_{i=1}^{k} \left\{ \bar{\boldsymbol{Q}}^{(i-1)} \boldsymbol{h}^{(i-1)}(z_{i-1}) - \bar{\boldsymbol{Q}}^{(i)} \boldsymbol{h}^{(i)}(z_{i-1}) + \left( \boldsymbol{\alpha}^{(i)} - \boldsymbol{\alpha}^{(i-1)} \right) z_{i-1} \right\}. \quad (45)$$

The final expression for $\sigma_z^{(k)}$ is established by substituting the layerwise integration constants of Eq. (44) back into Eq. (43). Thus,

$$\sigma_z^{(k)} = \nabla^\top \boldsymbol{D}^\top \left[ \left\{ \bar{\boldsymbol{Q}}^{(k)} \boldsymbol{h}^{(k)}(z) - \boldsymbol{\alpha}^{(k)} z + \boldsymbol{\beta}^{(k)} \right\} \boldsymbol{s}\mathcal{F} \right] - \nabla^\top \hat{T}_b \left( z - z_0 \right) + \hat{P}_b. \quad (46)$$

In the derivation of the layerwise integration constants of Eq. (44), the surface traction $\hat{P}_t$ on the top surface is not enforced explicitly. As the proof below shows, this condition is automatically satisfied if equilibrium of the transverse shear stress field Eq. (33) and transverse normal stress Eq. (46) is enforced. As we are dealing with an equivalent single layer, Cauchy's transverse equilibrium equation is integrated through the thickness to give

$$\int_{-t/2}^{t/2} \left( \nabla^\top \tau^{(k)} + \frac{\partial \sigma_z^{(k)}}{\partial z} \right) \mathrm{d}z = \nabla^\top \mathcal{Q} + \hat{P}_t - \hat{P}_b = 0 \quad (47)$$

where $\mathcal{Q} = (Q_{xz}, Q_{yz})$ are the transverse shear forces, and the substitutions $\hat{P}_t = \sigma_z^{(N_l)}(z_{N_l})$ and $\hat{P}_b = \sigma_z^{(1)}(z_0)$ have been made. An expression for $\nabla^\top \mathcal{Q}$ is derived by taking the divergence of $\tau^{(k)}$ in Eq. (33) and integrating in the z-direction. Thus,

$$\begin{aligned}\nabla^\top \mathcal{Q} &= \int_{-t/2}^{t/2} \nabla^\top \tau^{(k)} \mathrm{d}z \\ &= \nabla^\top \boldsymbol{D}^\top \sum_{k=1}^{N_l} \left[ \left\{ \bar{\boldsymbol{Q}}^{(k)} \left( \boldsymbol{h}^{(k)}(z_{k-1}) - \boldsymbol{h}^{(k)}(z_k) \right) + \boldsymbol{\alpha}^{(k)} t^{(k)} \right\} \boldsymbol{s}\mathcal{F} \right] + \nabla^\top \hat{T}_b \sum_{k=1}^{N_l} t^{(k)} \end{aligned} \quad (48)$$

where $t^{(k)}$ is the thickness of the $k^{th}$ layer. Next, an expression for $\hat{P}_t$, which was the only traction not enforced explicitly in the computation of the integration constants of Eq. (44) is found by substituting $z = z_{N_l}$ into the expression for $\sigma_z^{(k)}$ of Eq. (46),

$$\sigma_z^{(N_l)}(z_{N_l}) = \nabla^\top \boldsymbol{D}^\top \left[ \left\{ \bar{\boldsymbol{Q}}^{(N_l)} \boldsymbol{h}^{(N_l)}(z_{N_l}) - \boldsymbol{\alpha}^{(N_l)} z_{N_l} + \boldsymbol{\beta}^{(N_l)} \right\} \boldsymbol{s}\mathcal{F} \right] - \nabla^\top \hat{T}_b \left( z_{N_l} - z_0 \right) + \hat{P}_b$$

$$\hat{P}_t = \nabla^\top \boldsymbol{D}^\top \sum_{k=1}^{N_l} \left[ \left\{ \bar{\boldsymbol{Q}}^{(k)} \left( \boldsymbol{h}^{(k)}(z_k) - \boldsymbol{h}^{(k)}(z_{k-1}) \right) - \boldsymbol{\alpha}^{(k)} t^{(k)} \right\} \boldsymbol{s}\mathcal{F} \right] - \nabla^\top \hat{T}_b \sum_{k=1}^{N_l} t^{(k)} + \hat{P}_b. \quad (49)$$

By consideration of Eq. (48), the above Eq. (49) is transformed into

$$\hat{P}_t = -\nabla^\top \mathcal{Q} + \hat{P}_b \quad (50)$$

such that by substituting Eq. (50) back into Cauchy's single-layer equilibrium Eq. (47),

$$\nabla^\top \mathcal{Q} + \left( -\nabla^\top \mathcal{Q} + \hat{P}_b \right) - \hat{P}_b = 0. \quad (51)$$

Hence, the expression in Eq. (51) is satisfied identically. This is the second significant characteristic of the present higher-order model; as long as Eq. (47) is enforced when deriving the governing field equations and boundary conditions from a variational statement, equilibrium of the interfacial and surface normal tractions is automatically enforced *a priori* using the stress assumptions of Eqs. (27), (33) and (46).

Finally, the layerwise coefficients in the expression for $\sigma_z^{(k)}$ in Eq. (46) are conveniently combined into a single layerwise array $\boldsymbol{d}^{(k)}(z)$ such that

$$\sigma_z^{(k)} = \nabla^\top \boldsymbol{D}^\top \left[ \boldsymbol{d}^{(k)} \boldsymbol{s}\mathcal{F} \right] - \nabla^\top \hat{T}_b \left( z - z_0 \right) + \hat{P}_b. \quad (52)$$

## 6. Governing equations from the Hellinger-Reissner mixed-variational statement

In the HR mixed-variational statement, the Principle of Minimum Complementary Energy functional is enhanced by enforcing Cauchy's equilibrium equations and natural boundary conditions using displacement Lagrange multipliers. Hence,

$$\Pi_{HR}(\boldsymbol{u}, \boldsymbol{\sigma}) = \int_V U_0^*(\sigma_{ij}) \mathrm{d}V - \int_{S_1} \hat{u}_i t_i \mathrm{d}S + \int_V u_i \left( \sigma_{ij,j} + f_i \right) \mathrm{d}V - \int_{S_2} u_i \left( t_i - \hat{t}_i \right) \mathrm{d}S \quad (53)$$

where $U_0^*(\sigma_{ij})$ is the complementary energy density expressed in terms of the Cauchy stress tensor $\sigma_{ij}$, and the displacements $u_i$ are the Lagrange multipliers that enforce Cauchy's equilibrium equations $\sigma_{ij,j} + f_i$ in a variational sense throughout the volume of the continuum and the traction boundary conditions $t_i - \hat{t}_i$ on the boundary surface $S_2$. The tractions $t_i = \sigma_{ij} n_j = (\sigma_{nx}, \sigma_{ny}, \sigma_{nz})$ are the tractions in the $(x, y, z)$ directions acting on the boundary surface with outward normal $\boldsymbol{n} = (n_x, n_y, n_z)$.

In the present work, the model assumption of the inplane displacements is given by Eq. (13), i.e. $(u_x, u_y) = \boldsymbol{f}_u^{(k)} \mathcal{U}$, whereas the transverse displacement $u_z = w_0$ is constant throughout the thickness. Thus, the term associated with Cauchy's equilibrium equations in the HR functional in the absence of body forces is expressed as

$$\Pi_{\mathcal{L}} = \int_V u_i \sigma_{ij,j} \mathrm{d}V = \int_V \left[ \mathcal{U}^\top \boldsymbol{f}_u^{(k)^\top} \left( \boldsymbol{D}^\top \sigma^{(k)} + \frac{\partial \tau^{(k)}}{\partial z} \right) + w_0 \left( \nabla^\top \tau^{(k)} + \frac{\partial \sigma_z^{(k)}}{\partial z} \right) \right] \mathrm{d}V \quad (54)$$

where all quantities are defined as in the previous two sections. Taking the first variation of this functional with respect to the displacement variables, i.e. $\delta\mathcal{U}$ and $\delta w_0$, gives the higher-order equilibrium equations of the theory. For example, by integrating the first term in Eq. (54) by parts in the $z$-direction and taking the first variation with respect to the displacement variables $\mathcal{U}$ we have

$$\begin{aligned}\delta\Pi_{\mathcal{L}_1} &= \iiint \delta\mathcal{U}^\top \left( \boldsymbol{f}_u^{(k)^\top} \boldsymbol{D}^\top \sigma^{(k)} - \frac{\partial \boldsymbol{f}_u^{(k)^\top}}{\partial z} \tau^{(k)} \right) \mathrm{d}z\mathrm{d}y\mathrm{d}x \\ &\quad + \iint \delta\mathcal{U}^\top\, \boldsymbol{f}_u^{(k)^\top} \tau^{(k)} \Big|_{-t/2}^{t/2} \mathrm{d}y\mathrm{d}x \\ \delta\Pi_{\mathcal{L}_1} &= \iint \delta\mathcal{U}^\top \Big[ \boldsymbol{D}^F \mathcal{F}^* - \mathcal{T} + \boldsymbol{f}_u^{(N_l)^\top}(z_{N_l}) \hat{T}_t - \boldsymbol{f}_u^{(1)^\top}(z_0) \hat{T}_b \Big] \mathrm{d}y\mathrm{d}x \quad (55)\end{aligned}$$

where we have made use of Eq. (22) that the stress resultants $\mathcal{F}$ are the $z$-direction integrals of the in-plane stresses $\sigma^{(k)}$ multiplied by through-thickness shape functions. The vector of stress resultants $\mathcal{F}^*$ used in Eq. (55) is the same as $\mathcal{F}$ defined in Eq. (22) but does not contain the stress resultants associated with the derivatives of the ZZ function $\phi_{,i}^{(k)}$, i.e. $M_x^{\partial\phi}$ and $M_y^{\partial\phi}$, as these do not feature in $\boldsymbol{f}_u^{(k)}$. Furthermore, $\boldsymbol{D}^F = \boldsymbol{I}_{N_o} \otimes \boldsymbol{D}^\top$ with $\otimes$ denoting the Kronecker matrix product[1] and $\boldsymbol{I}_{N_o}$ a $(N_o+2)\times(N_o+2)$ identity matrix. Thus,

$$\boldsymbol{D}^F \mathcal{F}^* = \int_{-t/2}^{t/2} \boldsymbol{f}_u^{(k)^\top} \boldsymbol{D}^\top \sigma^{(k)} \mathrm{d}z. \quad (56)$$

Finally, a vector of transverse shear stress resultants, i.e. a vector of higher-order transverse shear forces $\mathcal{T} = (0, 0, Q_x, Q_y, \ldots, Q_x^\phi, Q_y^\phi)$ that balances the gradients of the stress resultants $\mathcal{F}^*$ in the higher-order equilibrium equations, has been defined as follows:

$$\mathcal{T} = \int_{-t/2}^{t/2} \frac{\partial \boldsymbol{f}_u^{(k)^\top}}{\partial z} \tau^{(k)} \mathrm{d}z. \quad (57)$$

When the first variation is set to zero, the term in square brackets of Eq. (55) represents the collection of equilibrium equations of the equivalent single-layer expressed as an array. These are the same higher-order equilibrium equations that are derived from the assumed displacement field Eq. (13) if the PVD is applied. For clarity, the equilibrium equations and associated Lagrange multipliers for a theory with $N_o = 1$ and ZZ functionality are

$$\begin{aligned}&\delta u_{x_0}: N_{x,x} + N_{xy,y} + \hat{T}_{tx} - \hat{T}_{bx} = 0 \\ &\delta u_{y_0}: N_{xy,x} + N_{y,y} + \hat{T}_{ty} - \hat{T}_{by} = 0 \\ &\delta u_{x_1}: M_{x,x} + M_{xy,y} - Q_x + z_{N_l}\hat{T}_{tx} - z_0 \hat{T}_{bx} = 0 \\ &\delta u_{y_1}: M_{xy,x} + M_{y,y} - Q_y + z_{N_l}\hat{T}_{ty} - z_0 \hat{T}_{by} = 0 \\ &\delta u_x^\phi: M_{x,x}^\phi + M_{xy,y}^\phi - Q_x^\phi + \phi_x^{(N_l)}(z_{N_l})\hat{T}_{tx} - \phi_x^{(1)}(z_0)\hat{T}_{bx} = 0 \\ &\delta u_y^\phi: M_{xy,x}^\phi + M_{y,y}^\phi - Q_y^\phi + \phi_y^{(N_l)}(z_{N_l})\hat{T}_{ty} - \phi_y^{(1)}(z_0)\hat{T}_{by} = 0\end{aligned} \quad (58)$$

where the comma notation is used to denote differentiation; $(N_x, N_y, N_{xy})$, $(M_x, M_y, M_{xy})$ and $(Q_x, Q_y)$ are the classical membrane forces, bending moments and transverse shear forces respectively; and $(M_x^\phi, M_y^\phi, M_{xy}^\phi)$ and $(Q_x^\phi, Q_y^\phi, )$ are the ZZ bending moments and ZZ transverse shear forces, respectively.

For a general assumption of displacements $\boldsymbol{u}$ and stresses $\boldsymbol{\sigma}$, the entire set of higher-order equilibrium equations in the square brackets of Eq. (55) needs to be satisfied. However, in the present work, the in-plane stresses and transverse shear stresses are inherently equilibrated due to the *a priori* integration step in Cauchy's equilibrium equations. As shown in the following derivation, this means that the equilibrium equations within the square brackets of Eq. (55) are, in fact, automatically satisfied and do not need to be enforced in the variational statement.

Thus, returning to the definition of the transverse shear stress resultants and integrating by parts,

$$\begin{aligned}\mathcal{T} &= \int_{-t/2}^{t/2} \frac{\partial \boldsymbol{f}_u^{(k)^\top}}{\partial z} \tau^{(k)} \mathrm{d}z \\ &= \boldsymbol{f}_u^{(k)^\top} \tau^{(k)} \Big|_{-t/2}^{t/2} - \int_{-t/2}^{t/2} \boldsymbol{f}_u^{(k)^\top} \frac{\partial \tau^{(k)}}{\partial z} \mathrm{d}z. \end{aligned} \quad (59)$$

As the model assumption for the transverse shear stresses is derived exactly from Cauchy's equilibrium equations in Eq. (29), we can replace $\tau_{,z}^{(k)}$ with $-\boldsymbol{D}^\top \sigma^{(k)}$. Hence,

$$\mathcal{T} = \boldsymbol{f}_u^{(N_l)^\top}(z_{N_l}) \hat{T}_t - \boldsymbol{f}_u^{(1)^\top}(z_0) \hat{T}_b + \int_{-t/2}^{t/2} \boldsymbol{f}_u^{(k)^\top} \boldsymbol{D}^\top \sigma^{(k)} \mathrm{d}z \quad (60)$$

and by using the expression in Eq. (56)

$$\mathcal{T} = \boldsymbol{f}_u^{(N_l)^\top}(z_{N_l}) \hat{T}_t - \boldsymbol{f}_u^{(1)^\top}(z_0) \hat{T}_b + \boldsymbol{D}^F \mathcal{F}^*. \quad (61)$$

Thus, in consideration of Eq. (61), all equilibrium equations in the square brackets of Eq. (55) vanish identically when using the present equilibrated assumptions for in-plane stresses $\sigma^{(k)}$ Eq. (27) and transverse shear stresses

[1] If $\boldsymbol{A}$ is an $m \times n$ matrix and $\boldsymbol{B}$ is a $q \times r$ matrix, then the Kronecker matrix product $\boldsymbol{A} \otimes \boldsymbol{B}$ is the $mq \times nr$ block matrix $\boldsymbol{A} \otimes \boldsymbol{B} = \begin{bmatrix} A_{11}\boldsymbol{B} & \ldots & A_{1n}\boldsymbol{B} \\ \vdots & \ddots & \vdots \\ A_{m1}\boldsymbol{B} & \ldots & A_{mn}\boldsymbol{B} \end{bmatrix}$.

$\tau^{(k)}$ Eq. (33), and therefore need not be enforced in the HR principle via Lagrange multipliers.

However, as discussed in Sections 4 and 5, equilibrium of the membrane forces $\mathcal{N} = (N_x, N_y, N_{xy})$ with the applied surface shear tractions, and equilibrium of the transverse shear forces $\mathcal{Q} = (Q_x, Q_y)$ with the applied surface normal tractions, has to be enforced to guarantee that the tractions on the top surface are recovered accurately. Therefore, a new set of governing equations for linear plate stretching and bending is derived by means of a *contracted* HR principle with only the membrane equilibrium Eq. (34) and bending equilibrium Eq. (47) enforced via Lagrange multipliers $\boldsymbol{u} = (u_{x_0}, u_{y_0}, w_0)$. Thus,

$$\begin{aligned}\Pi(\boldsymbol{u},\mathcal{F}) = &\int_V U_0^*(\mathcal{F})\mathrm{d}V - \int_{S_1} \hat{u}_i t_i \mathrm{d}S + \\ &\iint \begin{bmatrix} u_{x_0} & u_{y_0}\end{bmatrix} \left(\boldsymbol{D}^\top \mathcal{N} + \hat{T}_t - \hat{T}_b\right) \mathrm{d}y\mathrm{d}x + \\ &\iint w_0 \left(\nabla^\top \mathcal{Q} + \hat{P}_t - \hat{P}_b\right) \mathrm{d}y\mathrm{d}x - \\ &\int_{S_2} u_i \left(t_i - \hat{t}_i\right) \mathrm{d}S, \quad \text{for} \quad i,j = x,y,z. \end{aligned} \tag{62}$$

As observed by other authors, such as Batra et al. [28, 29], enforcing the equilibrium equations in the variational statement is a powerful technique for predicting accurate 3D stress fields in multilayered structures in a variationally consistent manner. However, the present *contracted* HR functional results in a structural model with fewer degree of freedom than the generalised model by Batra et al. as the in-plane and transverse shear stresses are based on the same degrees of freedom and fewer displacement Lagrange multipliers are needed. A possible disadvantage of this approach is that the reduction of variables leads to a loss in fidelity or general applicability of the model. However, this is offset by a considerable reduction in computational cost due to fewer equilibrium equations and variables.

For a linear elastic body with a predefined constitutive relation, the complementary energy density is expressed in terms of $\sigma_{ij}$ and the compliance tensor $S_{ijkl}$. Hence,

$$U_0^*(\sigma_{ij}) = \frac{1}{2} S_{ijkl}\sigma_{ij}\sigma_{kl}. \tag{63}$$

In previous work [31] it was found that the transverse normal stress is at least one order of magnitude smaller than the in-plane and transverse shear stresses for practical engineering laminates under classical load cases. Thus, the effect of transverse normal stresses is henceforth assumed to be small. Therefore, the contribution of $\sigma_z$ in the complementary energy density Eq. (63) is ignored, such that for a structure comprising monoclinic laminae we can write

$$U_0^*(\mathcal{F}) = \frac{1}{2}\sigma^{(k)^\top} \bar{\boldsymbol{Q}}^{(k)^{-1}} \sigma^{(k)} + \frac{1}{2}\tau^{(k)^\top} \boldsymbol{G}^{(k)^{-1}} \tau^{(k)} \tag{64}$$

where the in-plane stresses and transverse shear stresses are defined in Eqs. (27) and (39), respectively, $\bar{\boldsymbol{Q}}$ is the transformed reduced stiffness matrix for plane stress in $z$ as defined in Eq. (21), and the transverse shear constitutive matrix is given by

$$\boldsymbol{G}^{(k)} = \begin{bmatrix} C_{55} & C_{54} \\ C_{45} & C_{44} \end{bmatrix}^{(k)} \tag{65}$$

where $C_{55} = G_{xz}$, $C_{44} = G_{yz}$, and $C_{54} = C_{45}$ are the coupling terms between the two orthogonal transverse shear deformations. For orthotropic $0^\circ$ and $90^\circ$ lamina $C_{54} = C_{45} = 0$, whereas for general angle-ply laminae $C_{54} = C_{45} \neq 0$. As indicated by Eq. (64), once the substitutions for $\sigma^{(k)}$ and $\tau^{(k)}$ have been made from Eqs. (27) and (39), respectively, the complementary energy density is a function of the stress resultants $\mathcal{F}$ only. Note that even though the transverse normal stress $\sigma_z^{(k)}$ is ignored in the complementary energy density Eq. (64), the transverse normal stress is readily calculated from the model assumption Eq. (52) once the stress resultant field $\mathcal{F}$ is computed.

For equilibrium of the system, the first variation of the functional $\Pi$ in Eq. (62) must vanish identically, i.e.

$$\delta\Pi(\boldsymbol{u},\mathcal{F}) = 0.$$

Thus, by substituting Eq. (64) back into the contracted HR functional of Eq. (62) and taking the first variation,

$$\begin{aligned}\delta\Pi(\boldsymbol{u},\mathcal{F}) = \delta \Bigg[&\int_V \left\{\frac{1}{2}\sigma^{(k)^\top} \bar{\boldsymbol{Q}}^{(k)^{-1}} \sigma^{(k)} + \frac{1}{2}\tau^{(k)^\top} \boldsymbol{G}^{(k)^{-1}} \tau^{(k)}\right\} \mathrm{d}V + \\ &\iint \left\{\begin{bmatrix} u_{x_0} & u_{y_0}\end{bmatrix} \left(\boldsymbol{D}^\top \mathcal{N} + \hat{T}_t - \hat{T}_b\right) + w_0 \left(\nabla^\top \mathcal{Q} + \hat{P}_t - \hat{P}_b\right)\right\} \mathrm{d}y\mathrm{d}x - \\ &\int_{S_1} \left(\hat{u}_x t_x + \hat{u}_y t_y + \hat{u}_z t_z\right) \mathrm{d}S - \int_{S_2} \left\{u_x \left(t_x - \hat{t}_x\right) + u_y \left(t_y - \hat{t}_y\right) + u_z \left(t_z - \hat{t}_z\right)\right\} \mathrm{d}S\Bigg] = 0. \end{aligned} \tag{66}$$

The new set of governing equations is derived by substituting the stress fields for $\sigma^{(k)}$ and $\tau^{(k)}$ from Eqs. (27) and (39) into Eq. (66) and expanding the first variation. The corresponding Euler-Lagrange field equations in terms of the functional unknowns $\boldsymbol{u}$ and $\mathcal{F}$ are

$$\delta\left[u_{x_0}\ u_{y_0}\right] : \boldsymbol{D}^\top \mathcal{N} + \hat{T}_t - \hat{T}_b = \boldsymbol{0} \tag{67a}$$

$$\delta w_0 : \nabla^\top \boldsymbol{D}^\top \mathcal{M} + \nabla^\top \left(z_{N_l}\hat{T}_t - z_0\hat{T}_b\right) + \hat{P}_t - \hat{P}_b = 0 \tag{67b}$$

$$\delta\mathcal{F}^\top : (\boldsymbol{s}+\boldsymbol{\eta})\,\mathcal{F} + \boldsymbol{\eta}_x\frac{\partial\mathcal{F}}{\partial x} + \boldsymbol{\eta}_y\frac{\partial\mathcal{F}}{\partial y} + \boldsymbol{\eta}_{xx}\frac{\partial^2\mathcal{F}}{\partial x^2} + \boldsymbol{\eta}_{xy}\frac{\partial^2\mathcal{F}}{\partial x\partial y} + \boldsymbol{\eta}_{yy}\frac{\partial^2\mathcal{F}}{\partial y^2} + \boldsymbol{\chi}\hat{T}_b + \boldsymbol{\chi}_x\frac{\partial\hat{T}_b}{\partial x} + \boldsymbol{\chi}_y\frac{\partial\hat{T}_b}{\partial y} + \mathcal{L}_{eq} = \boldsymbol{0} \tag{67c}$$

where $\mathcal{N}$ and $\mathcal{M}$ are the classical membrane forces and bending moments, respectively, and are the first two subsets of the full stress resultant vector $\mathcal{F}$. The pertinent essential and natural boundary conditions are given by

$$\text{on } C_1 \quad \begin{cases} \delta\mathcal{F}_{bc}^\top : \boldsymbol{\eta}^{bc}\mathcal{F} + \boldsymbol{\eta}_x^{bc}\dfrac{\partial\mathcal{F}}{\partial x} + \boldsymbol{\eta}_y^{bc}\dfrac{\partial\mathcal{F}}{\partial y} + \boldsymbol{\chi}^{bc}\hat{T}_b + \mathcal{L}_{bc} = \hat{\mathcal{U}}_{bc} \\ \delta Q_{nz} : w_0 = \hat{w}_0 \end{cases} \tag{68a}$$

$$\text{on } C_2 \quad \delta\mathcal{U}_{bc}^\top :\ \mathcal{F}_{bc}^* = \hat{\mathcal{F}}_{bc}^* \quad \text{and} \quad \delta w_0 :\ Q_{nz} = \hat{Q}_{nz} \tag{68b}$$

where $\mathcal{F}_{bc} = (N_n, N_{ns}, M_n, M_{ns}, \dots)$ is the column vector of stress resultants transformed to the local normal-tangential coordinate system $(n,s,z)$ of the boundary curve $\Gamma$, $Q_{nz}$ is the transverse shear force acting normal to the boundary surface of the perimeter, and $\hat{\mathcal{U}}_{bc} = \left(\hat{u}_{n_0}, \hat{u}_{s_0}, \hat{u}_{n_1}, \hat{u}_{s_1}, \dots, \hat{u}_n^\phi, \hat{u}_s^\phi, 0, 0\right)$ is a column vector of prescribed displacement variables on the boundary. Similarly, $\mathcal{F}_{bc}^*$ is the stress resultant vector previously defined in Eq. (56), which is the same as $\mathcal{F}$ without the stress resultants associated with $\phi_{,i}^{(k)}$, i.e. $M_x^{\partial\phi}$ and $M_y^{\partial\phi}$, transformed to the local normal-tangential coordinate system $(n,s,z)$ of the boundary curve.

The governing field equations related to $\delta\left[u_{x_0}\quad u_{y_0}\right]$ and $\delta\mathcal{F}^\top$ are expressed as an array with each row defining a separate equation. The equations related to $\boldsymbol{\delta u}$ are the classical in-plane membrane and bending equilibrium equations. These equilibrium equations are supplemented by "enhanced" constitutive equations from $\delta\mathcal{F}^\top$ in Eqs. (67c). In these equations, the well-known constitutive equations of CLA expressed in inverted form, i.e.

$$\begin{Bmatrix} \epsilon_0 \\ \kappa \end{Bmatrix} = \begin{bmatrix} \boldsymbol{A} & \boldsymbol{B} \\ \boldsymbol{B} & \boldsymbol{D} \end{bmatrix}^{-1} \begin{Bmatrix} \mathcal{N} \\ \mathcal{M} \end{Bmatrix} = \boldsymbol{s}\mathcal{F}, \tag{69}$$

are enhanced with differential terms of the stress resultants $\mathcal{F}$, where $\mathcal{F}$ may also include higher-order moments beyond $\mathcal{N}$ and $\mathcal{M}$. Thus, all $\mathcal{O}\times\mathcal{O}$ matrices $\boldsymbol{\eta}$ in Eqs. (67c) are collections of transverse shear correction factors that, when multiplied by their corresponding higher-order moment terms $\dfrac{\partial^n\mathcal{F}}{\partial x_i^n}$, correct the product of the direct $\mathcal{O}\times\mathcal{O}$ compliance matrix $\boldsymbol{s}$ and moments $\mathcal{F}$. Similarly, the $\mathcal{O}\times 2$ matrices $\boldsymbol{\chi}$ are correction factors related to the applied surface shear tractions. In general, the addition of the superscript $bc$ to any matrix denotes correction factors that are applicable to the boundary curve $\Gamma$ and therefore include the outward normal vector $\boldsymbol{n} = (n_x, n_y)$.

Finally, $\mathcal{L}_{eq}$ is a $\mathcal{O}\times 1$ column vector that only includes derivatives of the Lagrange multipliers $\boldsymbol{u} = (u_{x_0}, u_{y_0}, w_0)$ and captures the reference surface stretching strains $\epsilon_0$ and curvatures $\kappa$,

$$\mathcal{L}_{eq} = -\begin{Bmatrix} \epsilon_0 \\ \kappa \\ \boldsymbol{0} \end{Bmatrix} \tag{70}$$

where

$$\epsilon_0 = \begin{bmatrix} \dfrac{\partial u_{x_0}}{\partial x} & \dfrac{\partial u_{y_0}}{\partial y} & \dfrac{\partial u_{x_0}}{\partial y} + \dfrac{\partial u_{y_0}}{\partial x} \end{bmatrix}^\top$$

$$\kappa = \begin{bmatrix} -\dfrac{\partial^2 w_0}{\partial x^2} & -\dfrac{\partial^2 w_0}{\partial y^2} & -2\dfrac{\partial^2 w_0}{\partial x\partial y} \end{bmatrix}^\top.$$

Similarly, $\mathcal{L}_{bc}$ is a $\mathcal{O}\times 1$ column vector that includes the transformed Lagrange multipliers $u_{n_0} = n_x u_{x_0} + n_y u_{y_0}$, $u_{s_0} = -n_y u_{x_0} + n_x u_{y_0}$ and rotations $\dfrac{\partial w_0}{\partial n}$ and $\dfrac{\partial w_0}{\partial s}$ of the boundary perimeter $\Gamma$,

$$\mathcal{L}_{bc} = \begin{bmatrix} u_{n_0} & u_{s_0} & -\dfrac{\partial w_0}{\partial n} & -\dfrac{\partial w_0}{\partial s} & 0 & \dots \end{bmatrix}^\top. \tag{71}$$

Thus, the physical significance of the displacement boundary conditions in Eq. (68a) is that Kirchhoff rotations normal and tangential to the boundary curve $\dfrac{\partial w_0}{\partial n}$ and $\dfrac{\partial w_0}{\partial s}$, respectively, are modified by transverse shear rotations. Therefore, the static inconsistency that occurs for Levinson-Reddy-type models discussed in reference [16] does not arise here, because the slope of the middle surface of the plate can change at a clamped boundary.

The full derivation of the governing equations, including details of all transverse shear correction coefficients, are given in Appendix A. The governing field equations Eq. (67) and boundary conditions Eq. (68) above are applicable to any multilayered laminate comprising linear elastic anisotropic laminae. Therefore, the HR model derived herein is applicable to straight-fibre and tow-steered composites as well as isotropic single-layer plates or multilayered ceramic structures such as laminated glass. For plates with material properties invariant of the planar $(x,y)$ directions, the governing equations simplify considerably as any terms involving planar derivatives vanish. Thus, for straight-fibre laminates and isotropic plates $\boldsymbol{\eta} = \boldsymbol{\eta}_x = \boldsymbol{\eta}_y = \boldsymbol{\chi} = \boldsymbol{\eta}^{bc} = \boldsymbol{0}$.

## 7. Conclusions

We have presented a computationally efficient, higher-order model for the bending and stretching of laminated plates using a contracted version of the HR functional. Our derivation is based on the notion that accurate transverse shear and transverse normal stress fields can be derived by integrating the in-plane stresses of displacement-based, higher-order theories in Cauchy's equilibrium equations.

By expanding the in-plane displacement field as a Taylor series of the through-thickness variable $z$, a higher-order in-plane stress field in terms of stress resultants was defined in Section 3. This higher-order in-plane stress field is then used to derive equilibrated transverse stresses from Cauchy's equilibrium equations in Sections 4 and 5. The derived transverse stress field assumptions are mathematically guaranteed to satisfy all interfacial and surface traction equilibrium conditions if the classical membrane and bending equilibrium equations are obeyed. This requirement naturally makes the HR principle an attractive variational statement, as the HR functional enforces the entire set of higher-order equilibrium equations of the equivalent single layer via Lagrange multipliers. As the 3D stress field assumptions in the present model are inherently equilibrated, all equilibrium equations of the equivalent single-layer are indeed satisfied *a priori* such that only the classical membrane and bending equations need to be enforced as constraints to recover the correct interfacial and surface tractions. This contracted HR-type functional is used to derive a new set of governing field equations and boundary conditions with the advantage that the number of variables in the model is greatly reduced compared to the case of independent stress field assumptions. Specifically, for an expansion of the in-plane stress fields up to the order of $z^{N_o}$, the ensuing reduction in the number of Lagrange multipliers is $2N_o$. The computational cost is further reduced by using the same degrees of freedom for the in-plane and transverse stress fields.

Due to higher-order fidelity, the model can be applied to laminates comprising layers with structural properties that vary by multiple orders of magnitude and also to advanced composites with curvilinear fibre paths. Thus, our model is applicable for modelling the bending and stretching of plates with heterogeneity in all three dimensions. In the accompanying *Part II* of this work, the accuracy of our model is tested and compared against 3D elasticity solutions and 3D FEM models for a wide range of stacking sequences.

In the derivation presented herein, the strain energy contribution of the transverse normal stress is neglected. The validity of this assumption is explored further in the accompanying *Part II* of this work. Nevertheless, we would like to suggest two possible ways of incorporating the effects of transverse normal deformation if these effects are deemed to be significant. The first is to use the generalised approach presented by Batra and co-workers [28, 29] of assuming independent Taylor or Legendre series expansions for the six stress and three displacement fields. The drawback of this approach is that the number of variables increases significantly. To maintain the computational efficiency of shared variables presented herein, the normal displacement field for $u_z$ in Eq. (4) can also be expanded as a Taylor series in the same manner as $u_x$ and $u_y$. In this case, the vector of stress resultants $\mathcal{F}$ includes extra higher-order moments that capture the stretching in the normal direction, and its Poisson effect on the in-plane stresses. Once the expression for in-plane stresses incorporating the effects of transverse normal deformation has been established, the rest of the model derivation follows the outline presented in this paper.


## Acknowledgments

This work was supported by the Engineering and Physical Sciences Research Council through the EPSRC Centre for Doctoral Training in Advanced Composites [grant number EP/G036772/1] at the University of Bristol.


## Appendix A. Derivation of HR governing equations

The HR functional in Eq. (66) is split into separate components representing the potential of in-plane stresses $\Pi_\sigma$, transverse shear stresses $\Pi_\tau$, the potential of the work done on the boundary $\Pi_\Gamma$ and the potential of the Lagrange multipliers $\Pi_{\mathcal{L}}$. Substituting the pertinent expressions for in-plane and transverse shear stresses Eq. (27) and Eq. (39), respectively, into the functional of Eq. (66) yields

$$\delta\Pi(\boldsymbol{u},\mathcal{F}) = \delta\left\{\Pi_\sigma(\mathcal{F}) + \Pi_\tau(\mathcal{F}) + \Pi_{\mathcal{L}}(\boldsymbol{u},\mathcal{F}) + \Pi_\Gamma(\boldsymbol{u},\mathcal{F})\right\} \tag{A.1}$$

where

$$\begin{aligned}\Pi_\sigma &= \frac{1}{2}\int_V \sigma^{(k)^\top} \bar{\boldsymbol{Q}}^{(k)^{-1}} \sigma^{(k)} \mathrm{d}V \\ &= \frac{1}{2}\int_V \left(\bar{\boldsymbol{Q}}^{(k)} \boldsymbol{f}_\epsilon^{(k)} \boldsymbol{s}\mathcal{F}\right)^\top \bar{\boldsymbol{Q}}^{(k)^{-1}} \left(\bar{\boldsymbol{Q}}^{(k)} \boldsymbol{f}_\epsilon^{(k)} \boldsymbol{s}\mathcal{F}\right) \mathrm{d}V\end{aligned} \tag{A.2a}$$

$$\begin{aligned}\Pi_\tau &= \frac{1}{2}\int_V \tau^{(k)^\top} \boldsymbol{G}^{(k)^{-1}} \tau^{(k)} \mathrm{d}V \\ &= \frac{1}{2}\int_V \left\{\boldsymbol{D}^\top\left(\boldsymbol{c}^{(k)}\boldsymbol{s}\mathcal{F}\right) + \hat{T}_b\right\}^\top \boldsymbol{G}^{(k)^{-1}} \cdot \\ &\qquad \left\{\boldsymbol{D}^\top\left(\boldsymbol{c}^{(k)}\boldsymbol{s}\mathcal{F}\right) + \hat{T}_b\right\} \mathrm{d}V\end{aligned} \tag{A.2b}$$

$$\begin{aligned}\Pi_{\mathcal{L}} = \iint \Big\{ &\begin{bmatrix} u_{x_0} & u_{y_0}\end{bmatrix}\left(\boldsymbol{D}^\top\mathcal{N} + \hat{T}_t - \hat{T}_b\right) + \\ &w_0\left(\nabla^\top\mathcal{Q} + \hat{P}_t - \hat{P}_b\right)\Big\}\,\mathrm{d}y\mathrm{d}x\end{aligned} \tag{A.2c}$$

$$\Pi_\Gamma = -\int_{S_1} \left(\hat{u}_x t_x + \hat{u}_y t_y + \hat{u}_z t_z\right)\mathrm{d}S -$$

$$\int_{S_2} \left\{u_x\left(t_x-\hat{t}_x\right)+u_y\left(t_y-\hat{t}_y\right)+u_z\left(t_z-\hat{t}_z\right)\right\} \mathrm{d}S \tag{A.2d}$$

and for equilibrium, the condition

$$\delta\Pi(\boldsymbol{u},\mathcal{F}) = 0 \tag{A.3}$$

must hold.

Performing the variations on the functionals in Eqs. (A.2a)-(A.2d) following the rules of the calculus of variations results in the expressions given below. For the potential of in-plane stresses we have

$$\begin{aligned}
\delta\Pi_\sigma &= \delta\left\{\frac{1}{2}\iint \mathcal{F}^\top \boldsymbol{s}^\top\left(\int \boldsymbol{f}_\epsilon^{(k)^\top} \bar{\boldsymbol{Q}}^{(k)} \boldsymbol{f}_\epsilon^{(k)} \mathrm{d}z\right) \boldsymbol{s}\mathcal{F}\mathrm{d}y\mathrm{d}x\right\} \\
&= \delta\left\{\frac{1}{2}\iint \mathcal{F}^\top \boldsymbol{s}^\top \boldsymbol{S}\boldsymbol{s}\mathcal{F}\mathrm{d}y\mathrm{d}x\right\} \\
&= \delta\left\{\frac{1}{2}\iint \mathcal{F}^\top \boldsymbol{s}^\top \mathcal{F}\mathrm{d}y\mathrm{d}x\right\} \\
&= \iint \mathcal{F}^\top \boldsymbol{s}^\top \delta\mathcal{F}\mathrm{d}y\mathrm{d}x.
\end{aligned} \tag{A.4}$$

For the potential of transverse shear stresses with $\boldsymbol{q}^{(k)} = \boldsymbol{G}^{(k)^{-1}}$ we have

$$\begin{aligned}
\Pi_\tau &= \frac{1}{2}\int_V \left\{\boldsymbol{D}^\top\left(\boldsymbol{c}^{(k)}\boldsymbol{s}\mathcal{F}\right)+\hat{T}_b\right\}^\top \boldsymbol{q}^{(k)}\cdot \\
&\qquad \left\{\boldsymbol{D}^\top\left(\boldsymbol{c}^{(k)}\boldsymbol{s}\mathcal{F}\right)+\hat{T}_b\right\}\mathrm{d}V \\
\delta\Pi_\tau &= \int_V \left\{\boldsymbol{D}^\top\left(\boldsymbol{c}^{(k)}\boldsymbol{s}\mathcal{F}\right)+\hat{T}_b\right\}^\top \boldsymbol{q}^{(k)} \left\{\boldsymbol{D}^\top\left(\boldsymbol{c}^{(k)}\boldsymbol{s}\delta\mathcal{F}\right)\right\}\mathrm{d}V.
\end{aligned} \tag{A.5}$$

By using the alternative definition of $\tau^{(k)}$ in terms of the layerwise constitutive matrices $\boldsymbol{R}^{(k)}$, $\boldsymbol{R}_x^{(k)}$ and $\boldsymbol{R}_y^{(k)}$ of Eq. (42), i.e.

$$\tau^{(k)} = \left(\boldsymbol{D}^\top\boldsymbol{R}^{(k)}\right)\mathcal{F}+\boldsymbol{R}_x^{(k)}\frac{\partial\mathcal{F}}{\partial x}+\boldsymbol{R}_y^{(k)}\frac{\partial\mathcal{F}}{\partial y}+\hat{T}_b, \tag{A.6}$$

the variation of the transverse shear functional in Eq. (A.5) now reads

$$\begin{aligned}
\delta\Pi_\tau = \int_V \Bigg[\tau^{(k)^\top}\boldsymbol{q}^{(k)}\Bigg\{\left(\boldsymbol{D}^\top\boldsymbol{R}^{(k)}\right)\delta\mathcal{F}+\boldsymbol{R}_x^{(k)}\delta\frac{\partial\mathcal{F}}{\partial x} \\
+\boldsymbol{R}_y^{(k)}\delta\frac{\partial\mathcal{F}}{\partial y}\Bigg\}\Bigg]\mathrm{d}V.
\end{aligned} \tag{A.7}$$

Expanding Eq. (A.7) and collecting common terms of $\delta\mathcal{F}$ results in

$$\begin{aligned}
\delta\Pi_\tau = \int_V \Bigg[\tau^{(k)^\top}\boldsymbol{q}^{(k)}\left(\boldsymbol{D}^\top\boldsymbol{R}^{(k)}\right)\delta\mathcal{F}+ \\
\tau^{(k)^\top}\boldsymbol{q}^{(k)}\boldsymbol{R}_x^{(k)}\delta\frac{\partial\mathcal{F}}{\partial x}+\tau^{(k)^\top}\boldsymbol{q}^{(k)}\boldsymbol{R}_y^{(k)}\delta\frac{\partial\mathcal{F}}{\partial y}\Bigg]\mathrm{d}V.
\end{aligned} \tag{A.8}$$

Next, by performing integration by parts on the terms $\delta\frac{\partial\mathcal{F}}{\partial x}$ and $\delta\frac{\partial\mathcal{F}}{\partial y}$ in Eq. (A.8),

$$\begin{aligned}
\delta\Pi_\tau = \int_V \Bigg[\tau^{(k)^\top}\boldsymbol{q}^{(k)}\left(\boldsymbol{D}^\top\boldsymbol{R}^{(k)}\right)-\frac{\partial}{\partial x}\left\{\tau^{(k)^\top}\boldsymbol{q}^{(k)}\boldsymbol{R}_x^{(k)}\right\} \\
-\frac{\partial}{\partial y}\left\{\tau^{(k)^\top}\boldsymbol{q}^{(k)}\boldsymbol{R}_y^{(k)}\right\}\Bigg]\delta\mathcal{F}\mathrm{d}V + \\
\int_{S_1}\left[n_x\left\{\tau^{(k)^\top}\boldsymbol{q}^{(k)}\boldsymbol{R}_x^{(k)}\right\}+n_y\left\{\tau^{(k)^\top}\boldsymbol{q}^{(k)}\boldsymbol{R}_y^{(k)}\right\}\right]\delta\mathcal{F}\mathrm{d}S
\end{aligned} \tag{A.9}$$

where $n_x$ and $n_y$ are the $(x,y)$ components of the normal vector $\boldsymbol{n}$ to the boundary surface $S$. Thus, Eq. (A.9) shows that the variation of the transverse shear stresses is a function of the transverse shear stresses themselves multiplied by the layerwise constitutive matrices $\boldsymbol{R}^{(k)}$, $\boldsymbol{R}_x^{(k)}$ and $\boldsymbol{R}_y^{(k)}$ and their in-plane derivatives.

The boundary integral in Eq. (A.9) is simplified further by combining the normal vector components $n_x$ and $n_y$ into a single matrix term such that the constitutive $\boldsymbol{R}_x^{(k)}$ and $\boldsymbol{R}_y^{(k)}$ matrices can be combined back into $\boldsymbol{R}^{(k)}$ (see Eq. (40)). Hence,

$$\int_{S_1}\left[\tau^{(k)^\top}\boldsymbol{q}^{(k)}\left\{n_x\boldsymbol{R}_x^{(k)}+n_y\boldsymbol{R}_y^{(k)}\right\}\right]\delta\mathcal{F}\mathrm{d}S \tag{A.10}$$

is simplified by defining

$$\boldsymbol{n}_D = n_x\boldsymbol{I}_x+n_y\boldsymbol{I}_y = \begin{bmatrix} n_x & 0 & n_y \\ 0 & n_y & n_x \end{bmatrix} \tag{A.11}$$

such that Eq. (A.10) now reads

$$\int_{S_1}\left[\tau^{(k)^\top}\boldsymbol{q}^{(k)}\boldsymbol{n}_D\boldsymbol{R}^{(k)}\right]\delta\mathcal{F}\mathrm{d}S. \tag{A.12}$$

In the boundary integral of Eq. (A.12) the virtual stress resultants in the column vector $\delta\mathcal{F}$ are defined in a global $(x,y)$ reference system. For example, the first six terms of $\mathcal{F}$ are the classical membrane forces $\mathcal{N} = (N_x, N_y, N_{xy})$ and bending moments $\mathcal{M} = (M_x, M_y, M_{xy})$. In order to transform the stress resultants in $\mathcal{F}$ from the global coordinate system $(x,y,z)$ to the local normal-tangential coordinate system $(n,s,z)$ of the boundary surface, the transformation matrix $\boldsymbol{T}$ is applied,

$$\begin{Bmatrix} F_x \\ F_y \\ F_{xy} \end{Bmatrix} = \boldsymbol{T}\begin{Bmatrix} F_n \\ F_s \\ F_{ns} \end{Bmatrix}, \ \boldsymbol{T} = \begin{bmatrix} n_x^2 & n_y^2 & -2n_xn_y \\ n_y^2 & n_x^2 & 2n_xn_y \\ n_xn_y & -n_xn_y & n_x^2-n_y^2 \end{bmatrix}. \tag{A.13}$$

After converting all stress resultants to the local normal-tangential coordinate system $(n,s,z)$, the orthogonality condition of $n$ and $s$ is used to conclude that the stress resultants $F_s$ can do no work normal to the boundary surface. Thus, the second column of $\boldsymbol{T}$ can be disregarded in the stress resultant transformation of $\delta F$, such that

$$\boldsymbol{T}_n = \begin{bmatrix} n_x^2 & -2n_x n_y \\ n_y^2 & 2n_x n_y \\ n_x n_y & n_x^2 - n_y^2 \end{bmatrix}. \tag{A.14}$$

The complete column vector of all stress resultants $\mathcal{F} = (N_x, N_y, N_{xy}, M_x, M_y, M_{xy}, \dots)$ is transformed into the boundary stress resultant $\mathcal{F}_{bc} = (N_n, N_{ns}, M_n, M_{ns}, \dots)$ as follows

$$\mathcal{F} = \boldsymbol{T}_{bc}\mathcal{F}_{bc} \quad \text{where} \quad \boldsymbol{T}_{bc} = \boldsymbol{I}_{\mathcal{O}} \otimes \boldsymbol{T}_n \tag{A.15}$$

where $\otimes$ is the Kronecker matrix product[2] and $\boldsymbol{I}_{\mathcal{O}}$ is the $\mathcal{O} \times \mathcal{O}$ identity matrix. Thus, Eq. (A.9) is rewritten to accommodate the new boundary integral,

$$\begin{aligned}\delta\Pi_\tau = \int_V &\left[\tau^{(k)^\top} \boldsymbol{q}^{(k)} \left(\boldsymbol{D}^\top \boldsymbol{R}^{(k)}\right) - \frac{\partial}{\partial x}\left\{\tau^{(k)^\top} \boldsymbol{q}^{(k)} \boldsymbol{R}_x^{(k)}\right\} \right.\\ &\left. - \frac{\partial}{\partial y}\left\{\tau^{(k)^\top} \boldsymbol{q}^{(k)} \boldsymbol{R}_y^{(k)}\right\}\right] \delta\mathcal{F}\mathrm{d}V + \\ &\int_{S_1} \left[\tau^{(k)^\top} \boldsymbol{q}^{(k)} \boldsymbol{n}_D \boldsymbol{R}^{(k)} \boldsymbol{T}_{bc}\right] \delta\mathcal{F}_{bc}\mathrm{d}S. \end{aligned} \tag{A.16}$$

Finally, all that remains is to expand the derivatives in Eq. (A.16) using the differential product rule and integrate in the $z$-direction to collapse the terms onto an equivalent single layer. Thus, by defining pertinent shear correction matrices in the final $z$-wise integration step, we arrive at

$$\begin{aligned}\delta\Pi_\tau = \iint &\left[\boldsymbol{\eta}\mathcal{F} + \boldsymbol{\eta}_x \frac{\partial \mathcal{F}}{\partial x} + \boldsymbol{\eta}_y \frac{\partial \mathcal{F}}{\partial y} + \boldsymbol{\eta}_{xx} \frac{\partial^2 \mathcal{F}}{\partial x^2} + \right.\\ &\left. \boldsymbol{\eta}_{xy} \frac{\partial^2 \mathcal{F}}{\partial x \partial y} + \boldsymbol{\eta}_{yy} \frac{\partial^2 \mathcal{F}}{\partial^2 y} + \boldsymbol{\chi}\hat{T}_b + \boldsymbol{\chi}_x \frac{\partial \hat{T}_b}{\partial x} + \boldsymbol{\chi}_y \frac{\partial \hat{T}_b}{\partial y}\right]^\top \delta\mathcal{F}\mathrm{d}y\mathrm{d}x \\ &+ \int_{C_1} \left[\boldsymbol{\eta}^{bc}\mathcal{F} + \boldsymbol{\eta}_x^{bc} \frac{\partial \mathcal{F}}{\partial x} + \boldsymbol{\eta}_y^{bc} \frac{\partial \mathcal{F}}{\partial y} + \boldsymbol{\chi}^{bc}\hat{T}_b\right]^\top \delta\mathcal{F}_{bc}\mathrm{d}s \end{aligned} \tag{A.17}$$

where all $\boldsymbol{\eta}_\alpha$ are $\mathcal{O} \times \mathcal{O}$ matrices of shear coefficients that automatically include pertinent shear correction factors. The $\mathcal{O} \times 2$ matrices $\boldsymbol{\chi}_\alpha$ are correction factors that enforce transverse shearing effects of the surface shear tractions. In each case the additional superscript $bc$ refers to coefficients used in the boundary conditions. The size of these matrices depends on the chosen order of the model $\mathcal{O}$. For example, a first-order shear theory has $\mathcal{O} = 6$ with membrane forces $\mathcal{N}$ and bending moments $\mathcal{M}$, i.e. $\mathcal{F} = (N_x, N_y, N_{xy}, M_x, M_y, M_{xy})$.

The transposes of the shear correction matrices $\boldsymbol{\eta}_\alpha^\top$ and $\boldsymbol{\chi}_\alpha^\top$ in the double integral are

$$\begin{aligned}\boldsymbol{\eta}^\top = \sum_{k=1}^{N_l} \int_{z_{k-1}}^{z_k} &\left[\left(\boldsymbol{D}^\top \boldsymbol{R}^{(k)}\right)^\top \left\{\boldsymbol{q}^{(k)} \left(\boldsymbol{D}^\top \boldsymbol{R}^{(k)}\right) - \right.\right.\\ &\left. \frac{\partial}{\partial x}\left(\boldsymbol{q}^{(k)} \boldsymbol{R}_x^{(k)}\right) - \frac{\partial}{\partial y}\left(\boldsymbol{q}^{(k)} \boldsymbol{R}_y^{(k)}\right)\right\} - \\ &\left. \frac{\partial}{\partial x}\left(\boldsymbol{D}^\top \boldsymbol{R}^{(k)}\right)^\top \boldsymbol{q}^{(k)} \boldsymbol{R}_x^{(k)} - \frac{\partial}{\partial y}\left(\boldsymbol{D}^\top \boldsymbol{R}^{(k)}\right)^\top \boldsymbol{q}^{(k)} \boldsymbol{R}_y^{(k)}\right] \mathrm{d}z \end{aligned} \tag{A.18a}$$

$$\begin{aligned}\boldsymbol{\eta}_x^\top = \sum_{k=1}^{N_l} \int_{z_{k-1}}^{z_k} &\left[\boldsymbol{R}_x^{(k)^\top} \left\{\boldsymbol{q}^{(k)} \left(\boldsymbol{D}^\top \boldsymbol{R}^{(k)}\right) - \right.\right.\\ &\left. \frac{\partial}{\partial x}\left(\boldsymbol{q}^{(k)} \boldsymbol{R}_x^{(k)}\right) - \frac{\partial}{\partial y}\left(\boldsymbol{q}^{(k)} \boldsymbol{R}_y^{(k)}\right)\right\} - \left(\boldsymbol{D}^\top \boldsymbol{R}^{(k)}\right)^\top \boldsymbol{q}^{(k)} \boldsymbol{R}_x^{(k)} \\ &\left. - \frac{\partial \boldsymbol{R}_x^{(k)^\top}}{\partial x} \boldsymbol{q}^{(k)} \boldsymbol{R}_x^{(k)} - \frac{\partial \boldsymbol{R}_x^{(k)^\top}}{\partial y} \boldsymbol{q}^{(k)} \boldsymbol{R}_y^{(k)}\right] \mathrm{d}z \end{aligned} \tag{A.18b}$$

$$\begin{aligned}\boldsymbol{\eta}_y^\top = \sum_{k=1}^{N_l} \int_{z_{k-1}}^{z_k} &\left[\boldsymbol{R}_y^{(k)^\top} \left\{\boldsymbol{q}^{(k)} \left(\boldsymbol{D}^\top \boldsymbol{R}^{(k)}\right) - \right.\right.\\ &\left. \frac{\partial}{\partial x}\left(\boldsymbol{q}^{(k)} \boldsymbol{R}_x^{(k)}\right) - \frac{\partial}{\partial y}\left(\boldsymbol{q}^{(k)} \boldsymbol{R}_y^{(k)}\right)\right\} - \left(\boldsymbol{D}^\top \boldsymbol{R}^{(k)}\right)^\top \boldsymbol{q}^{(k)} \boldsymbol{R}_y^{(k)} \\ &\left. - \frac{\partial \boldsymbol{R}_y^{(k)^\top}}{\partial x} \boldsymbol{q}^{(k)} \boldsymbol{R}_x^{(k)} - \frac{\partial \boldsymbol{R}_y^{(k)^\top}}{\partial y} \boldsymbol{q}^{(k)} \boldsymbol{R}_y^{(k)}\right] \mathrm{d}z \end{aligned} \tag{A.18c}$$

$$\boldsymbol{\eta}_{xx}^\top = -\sum_{k=1}^{N_l} \int_{z_{k-1}}^{z_k} \boldsymbol{R}_x^{(k)^\top} \boldsymbol{q}^{(k)} \boldsymbol{R}_x^{(k)} \mathrm{d}z \tag{A.18d}$$

$$\boldsymbol{\eta}_{yy}^\top = -\sum_{k=1}^{N_l} \int_{z_{k-1}}^{z_k} \boldsymbol{R}_y^{(k)^\top} \boldsymbol{q}^{(k)} \boldsymbol{R}_y^{(k)} \mathrm{d}z \tag{A.18e}$$

$$\boldsymbol{\eta}_{xy}^\top = -\sum_{k=1}^{N_l} \int_{z_{k-1}}^{z_k} \left[\boldsymbol{R}_x^{(k)^\top} \boldsymbol{q}^{(k)} \boldsymbol{R}_y^{(k)} + \boldsymbol{R}_y^{(k)^\top} \boldsymbol{q}^{(k)} \boldsymbol{R}_x^{(k)}\right] \mathrm{d}z \tag{A.18f}$$

$$\begin{aligned}\boldsymbol{\chi}^\top = \sum_{k=1}^{N_l} \int_{z_{k-1}}^{z_k} &\left[\boldsymbol{q}^{(k)} \left(\boldsymbol{D}^\top \boldsymbol{R}^{(k)}\right) - \frac{\partial}{\partial x}\left(\boldsymbol{q}^{(k)} \boldsymbol{R}_x^{(k)}\right) - \right.\\ &\left. \frac{\partial}{\partial y}\left(\boldsymbol{q}^{(k)} \boldsymbol{R}_y^{(k)}\right)\right] \mathrm{d}z \end{aligned} \tag{A.18g}$$

$$\boldsymbol{\chi}_x^\top = -\sum_{k=1}^{N_l} \int_{z_{k-1}}^{z_k} \boldsymbol{q}^{(k)} \boldsymbol{R}_x^{(k)} \mathrm{d}z \tag{A.18h}$$

$$\boldsymbol{\chi}_y^\top = -\sum_{k=1}^{N_l} \int_{z_{k-1}}^{z_k} \boldsymbol{q}^{(k)} \boldsymbol{R}_y^{(k)} \mathrm{d}z \tag{A.18i}$$

and in the boundary integral $\boldsymbol{\eta}_\alpha^{bc^\top}$ and $\boldsymbol{\chi}^{bc^\top}$ are given by

$$\boldsymbol{\eta}^{bc^\top} = \sum_{k=1}^{N_l} \int_{z_{k-1}}^{z_k} \left(\boldsymbol{D}^\top \boldsymbol{R}^{(k)}\right)^\top \boldsymbol{q}^{(k)} \boldsymbol{n}_D \boldsymbol{R}^{(k)} \boldsymbol{T}_{bc} \mathrm{d}z \tag{A.19a}$$

$$\boldsymbol{\eta}_x^{bc^\top} = \sum_{k=1}^{N_l} \int_{z_{k-1}}^{z_k} \boldsymbol{R}_x^{(k)^\top} \boldsymbol{q}^{(k)} \boldsymbol{n}_D \boldsymbol{R}^{(k)} \boldsymbol{T}_{bc} \mathrm{d}z \tag{A.19b}$$

[2] Defined on page 11.

$$\boldsymbol{\eta}_y^{bc^\top} = \sum_{k=1}^{N_l} \int_{z_{k-1}}^{z_k} \boldsymbol{R}_y^{(k)^\top} \boldsymbol{q}^{(k)} \boldsymbol{n}_D \boldsymbol{R}^{(k)} \boldsymbol{T}_{bc} \mathrm{d}z \tag{A.19c}$$

$$\boldsymbol{\chi}^{bc^\top} = \sum_{k=1}^{N_l} \int_{z_{k-1}}^{z_k} \boldsymbol{q}^{(k)} \boldsymbol{n}_D \boldsymbol{R}^{(k)} \boldsymbol{T}_{bc} \mathrm{d}z. \tag{A.19d}$$

The expressions in Eq. (A.18) and (A.19) are valid for any multilayered plate comprised of linear elastic anisotropic laminae. Thus, the expressions are applicable to straight-fibre and tow-steered composites, as well as for isotropic single-layer plates or multilayered ceramic structures such as laminated glass. For plates with material properties invariant of the planar $(x, y)$ directions, the expressions in Eq. (A.18) and (A.19) simplify considerably as any terms involving $\boldsymbol{D}^\top, \partial/\partial x, \partial/\partial y$ vanish. Thus, for straight-fibre laminates $\boldsymbol{\eta}^\top = \boldsymbol{\eta}_x^\top = \boldsymbol{\eta}_y^\top = \boldsymbol{\chi}^\top = \boldsymbol{\eta}^{bc^\top} = \boldsymbol{0}$.

The potential of the Lagrange multipliers Eq. (A.2c) is given by

$$\Pi_{\mathcal{L}} = \iint \left\{ \begin{bmatrix} u_{x_0} & u_{y_0} \end{bmatrix} \left( \boldsymbol{D}^\top \mathcal{N} + \hat{T}_t - \hat{T}_b \right) + w_0 \left( \nabla^\top \mathcal{Q} + \hat{P}_t - \hat{P}_b \right) \right\} \mathrm{d}y \mathrm{d}x. \tag{A.20}$$

An expression for the transverse shear stress resultants $\mathcal{Q} = (Q_{xz}, Q_{yz})$ in terms of bending moments $\mathcal{M}$ is found by using the bending moment equilibrium from Cauchy's in-plane equilibrium equations. Hence,

$$\int_{z_0}^{z_N} z \left( \boldsymbol{D}^\top \sigma^{(k)} + \frac{\partial \tau^{(k)}}{\partial z} \right) \mathrm{d}z = \boldsymbol{D}^\top \mathcal{M} + \int_{z_0}^{z_N} z \frac{\partial \tau^{(k)}}{\partial z} \mathrm{d}z = \boldsymbol{0}$$

and via integration by parts,

$$\begin{aligned} &\boldsymbol{D}^\top \mathcal{M} + \left[ z \tau^{(k)} \right]_{z_0}^{z_{N_l}} - \int_{z_0}^{z_N} \tau^{(k)} \mathrm{d}z = \boldsymbol{0} \\ &\boldsymbol{D}^\top \mathcal{M} + \left[ z_{N_l} \tau^{(N_l)}(z_{N_l}) - z_0 \tau^{(1)}(z_0) \right] - \mathcal{Q} = \boldsymbol{0} \\ &\therefore \mathcal{Q} = \boldsymbol{D}^\top \mathcal{M} + \left( z_{N_l} \hat{T}_t - z_0 \hat{T}_b \right). \end{aligned} \tag{A.21}$$

Note, that Eq. (A.21) is the expression seen in the third and fourth equations of Eq. (58). Substituting the expression for $\mathcal{Q}$ from Eq. (A.21) into Eq. (A.20) results in

$$\begin{aligned} \Pi_{\mathcal{L}} = &\iint \begin{bmatrix} u_{x_0} & u_{y_0} \end{bmatrix} \left( \boldsymbol{D}^\top \mathcal{N} + \hat{T}_t - \hat{T}_b \right) \mathrm{d}y \mathrm{d}x + \\ &\iint w_0 \left( \nabla^\top \boldsymbol{D}^\top \mathcal{M} + \nabla^\top \left( z_{N_l} \hat{T}_t - z_0 \hat{T}_b \right) + \hat{P}_t - \hat{P}_b \right) \mathrm{d}y \mathrm{d}x. \end{aligned} \tag{A.22}$$

Now, taking the first variation of Eq. (A.22),

$$\begin{aligned} \delta\Pi_{\mathcal{L}} = &\iint \left\{ \begin{bmatrix} \delta u_{x_0} & \delta u_{y_0} \end{bmatrix} \left( \boldsymbol{D}^\top \mathcal{N} + \hat{T}_t - \hat{T}_b \right) + \begin{bmatrix} u_{x_0} & u_{y_0} \end{bmatrix} \left( \boldsymbol{D}^\top \delta \mathcal{N} \right) \right\} \mathrm{d}y \mathrm{d}x + \\ &\iint \left\{ \delta w_0 \left( \nabla^\top \boldsymbol{D}^\top \mathcal{M} + \nabla^\top \left( z_{N_l} \hat{T}_t - z_0 \hat{T}_b \right) + \hat{P}_t - \hat{P}_b \right) + w_0 \left( \nabla^\top \boldsymbol{D}^\top \delta \mathcal{M} \right) \right\} \mathrm{d}y \mathrm{d}x \end{aligned} \tag{A.23}$$

and then integrating the expressions involving derivatives of $\delta\mathcal{N}$ and $\delta\mathcal{M}$ by parts we have

$$\begin{aligned} \delta\Pi_{\mathcal{L}} = &\iint \left\{ \begin{bmatrix} \delta u_{x_0} & \delta u_{y_0} \end{bmatrix} \left( \boldsymbol{D}^\top \mathcal{N} + \hat{T}_t - \hat{T}_b \right) - \left( \boldsymbol{D} \begin{Bmatrix} u_{x_0} \\ u_{y_0} \end{Bmatrix} \right)^\top \delta \mathcal{N} \right\} \mathrm{d}y \mathrm{d}x + \\ &\iint \left\{ \delta w_0 \left( \nabla^\top \boldsymbol{D}^\top \mathcal{M} + \nabla^\top \left( z_{N_l} \hat{T}_t - z_0 \hat{T}_b \right) + \hat{P}_t - \hat{P}_b \right) + \left( \nabla^\top \boldsymbol{D}^\top w_0 \right) \delta \mathcal{M} \right\} \mathrm{d}y \mathrm{d}x + \\ &\int_{C_1} \begin{bmatrix} u_{n_0} & u_{s_0} \end{bmatrix} \delta \mathcal{N}_{bc} \mathrm{d}s - \int_{C_1} \left( \nabla_{ns} w_0 \right)^\top \delta \mathcal{M}_{bc} \mathrm{d}s + \int_{C_1} w_0 \delta Q_{nz} \mathrm{d}s \end{aligned} \tag{A.24}$$

where $\nabla_{ns} = \left( \frac{\partial}{\partial n}, \frac{\partial}{\partial s} \right)$, $\mathcal{N}_{bc} = (N_n, N_{ns})$, $\mathcal{M}_{bc} = (M_n, M_{ns})$, $Q_{nz}$ is the transverse shear force acting on the normal boundary surface, and two new variables $u_{n_0} = n_x u_{x_0} + n_y u_{y_0}$ and $u_{s_0} = -n_y u_{x_0} + n_x u_{y_0}$ have been introduced to capture the displacement Lagrange multipliers on the boundary. In general, this transformation follows the rule

$$\begin{Bmatrix} \hat{e}_x \\ \hat{e}_y \end{Bmatrix} = \begin{bmatrix} n_x & -n_y \\ n_y & n_x \end{bmatrix} \begin{Bmatrix} \hat{e}_n \\ \hat{e}_s \end{Bmatrix} \tag{A.25}$$

where $\hat{\boldsymbol{e}}$ is a unit vector.

Finally, the first variation of the work done on the boundary surface $S$ of Eq. (A.2d) has to be evaluated. Thus,

$$\begin{aligned} \delta\Pi_\Gamma = &-\int_{S_1} \left( \hat{u}_x \delta t_x + \hat{u}_y \delta t_y + \hat{u}_z \delta t_z \right) \mathrm{d}S - \\ &\int_{S_2} \left\{ \delta u_x \left( t_x - \hat{t}_x \right) + \delta u_y \left( t_y - \hat{t}_y \right) + \delta u_z \left( t_z - \hat{t}_z \right) \right\} \mathrm{d}S. \end{aligned} \tag{A.26}$$

When the displacements are transformed from $(\hat{u}_x, \hat{u}_y, \hat{u}_z)$ to $(\hat{u}_n, \hat{u}_s, \hat{u}_z)$ and tractions transfomed from $(t_x, t_y, t_z) = (\sigma_{nx}, \sigma_{ny}, \sigma_{nz})$ to $(t_n, t_s, t_z) = (\sigma_{nn}, \sigma_{ns}, \sigma_{nz})$ using Eq. (A.25), the first variation of the work done on the boundary surface Eq. (A.26) reads

$$\begin{aligned} \delta\Pi_\Gamma = &-\int_{S_1} \left( \hat{u}_n \delta t_n + \hat{u}_s \delta t_s + \hat{u}_z \delta t_z \right) \mathrm{d}S - \\ &\int_{S_2} \left\{ \delta u_n \left( t_n - \hat{t}_n \right) + \delta u_s \left( t_s - \hat{t}_s \right) + \delta u_z \left( t_z - \hat{t}_z \right) \right\} \mathrm{d}S. \end{aligned} \tag{A.27}$$

Following the generalised displacement field for $u_x$ and $u_y$ of Eq. (4), the normal-tangential displacements $u_n$ and $u_s$ are expanded as follows:

$$u_n^{(k)}(n,s,z) = u_{n_0}(n,s) + z u_{n_1}(n,s) + z^2 u_{n_2}(n,s) + \dots + \phi_n^{(k)}(n,s,z) u_n^{\phi}(n,s) \quad \text{(A.28a)}$$

$$u_s^{(k)}(n,s,z) = u_{s_0}(n,s) + z u_{s_1}(n,s) + z^2 u_{s_2}(n,s) + \dots + \phi_s^{(k)}(n,s,z) u_s^{\phi}(n,s) \quad \text{(A.28b)}$$

$$u_z(n,s) = w_0. \quad \text{(A.28c)}$$

Writing Eq. (A.28) in a more concise matrix notation we have

$$\mathcal{U}_{ns}^{(k)} = \begin{Bmatrix} u_n^{(k)} \\ u_s^{(k)} \end{Bmatrix} = \begin{bmatrix} \boldsymbol{I}_2 & \boldsymbol{Z}_2 & \boldsymbol{Z}_2^2 & \dots \end{bmatrix} \begin{Bmatrix} \mathcal{U}_{0bc}^g \\ \mathcal{U}_{1bc}^g \\ \mathcal{U}_{2bc}^g \\ \vdots \end{Bmatrix} + \begin{bmatrix} \phi_n^{(k)} & 0 \\ 0 & \phi_s^{(k)} \end{bmatrix} \begin{Bmatrix} u_n^{\phi} \\ u_s^{\phi} \end{Bmatrix} \quad \text{(A.29)}$$

where $\boldsymbol{I}_2, \boldsymbol{Z}_2, \boldsymbol{Z}_2^2, \dots$ are as previously defined in Eq. (9) and

$$\mathcal{U}_{0bc}^g = \begin{bmatrix} u_{n_0} & u_{s_0} \end{bmatrix}^\top, \; \mathcal{U}_{1bc}^g = \begin{bmatrix} u_{n_1} & u_{s_1} \end{bmatrix}^\top, \; \mathcal{U}_{2bc}^g = \begin{bmatrix} u_{n_2} & u_{s_2} \end{bmatrix}^\top, \quad \dots \quad \text{(A.30)}$$

By defining,

$$\boldsymbol{f}_{ubc}^l = \begin{bmatrix} \phi_n^{(k)} & 0 \\ 0 & \phi_s^{(k)} \end{bmatrix}, \quad \mathcal{U}_{bc}^l = \begin{bmatrix} u_n^{\phi} & u_s^{\phi} \end{bmatrix}^\top, \quad \mathcal{U}_{bc}^g = \begin{bmatrix} \mathcal{U}_{0bc}^g & \mathcal{U}_{1bc}^g & \mathcal{U}_{2bc}^g & \dots \end{bmatrix}^\top \quad \text{(A.31)}$$

Eq. (A.29) now reads

$$\mathcal{U}_{ns}^{(k)} = \boldsymbol{f}_u^g \mathcal{U}_{bc}^g + \boldsymbol{f}_{ubc}^l \mathcal{U}_{bc}^l = \begin{bmatrix} \boldsymbol{f}_u^g & \boldsymbol{f}_{ubc}^l \end{bmatrix} \begin{Bmatrix} \mathcal{U}_{bc}^g \\ \mathcal{U}_{bc}^l \end{Bmatrix} = \boldsymbol{f}_{ubc}^{(k)} \mathcal{U}_{bc}. \quad \text{(A.32)}$$

Substituting Eq. (A.32) into the variation of the work done on the boundary Eq. (A.27) gives

$$\delta\Pi_\Gamma = -\int_{S_1} \left( \begin{bmatrix} \hat{u}_n & \hat{u}_s \end{bmatrix} \begin{Bmatrix} \delta t_n \\ \delta t_s \end{Bmatrix} + \hat{u}_z \delta t_z \right) \mathrm{d}S - \int_{S_2} \left( \begin{bmatrix} \delta u_n & \delta u_s \end{bmatrix} \begin{Bmatrix} t_n - \hat{t}_n \\ t_s - \hat{t}_s \end{Bmatrix} + \delta u_z \left( t_z - \hat{t}_z \right) \right) \mathrm{d}S$$

$$\delta\Pi_\Gamma = -\int_{S_1} \left( \hat{\mathcal{U}}_{bc}^\top \boldsymbol{f}_{ubc}^{(k)\top} \begin{Bmatrix} \delta\sigma_{nn} \\ \delta\sigma_{ns} \end{Bmatrix} + \hat{w}_0 \delta\sigma_{nz} \right) \mathrm{d}S - \int_{S_2} \left( \delta\mathcal{U}_{bc}^\top \boldsymbol{f}_{ubc}^{(k)\top} \begin{Bmatrix} \sigma_{nn} - \hat{\sigma}_{nn} \\ \sigma_{ns} - \hat{\sigma}_{ns} \end{Bmatrix} + \delta w_0 \left( \sigma_{nz} - \hat{\sigma}_{nz} \right) \right) \mathrm{d}S \quad \text{(A.33)}$$

and finally, by integrating in the $z$-direction

$$\delta\Pi_\Gamma = -\int_{C_1} \left( \hat{\mathcal{U}}_{bc}^\top \delta\mathcal{F}_{bc}^* + \hat{w}_0 \delta Q_{nz} \right) \mathrm{d}s - \int_{C_2} \left[ \delta\mathcal{U}_{bc}^\top \left( \mathcal{F}_{bc}^* - \hat{\mathcal{F}}_{bc}^* \right) + \delta w_0 \left( Q_{nz} - \hat{Q}_{nz} \right) \right] \mathrm{d}s \quad \text{(A.34)}$$

where $C_1$ and $C_2$ are the boundary curves corresponding to the intersections of the reference surface $\Omega$ with the boundary surfaces $S_1$ and $S_2$, respectively, and $Q_{nz}$ is the transverse shear force normal to the boundary. Furthermore, $\mathcal{F}_{bc}^*$ is the stress resultant vector without the stress resultants associated with $\phi_{,i}^{(k)}$, i.e. $M_x^{\partial\phi}$ and $M_y^{\partial\phi}$, transformed to the local normal-tangential coordinate system $(n,s,z)$ of the boundary curve. Thus, when combining the coefficient of $\delta\mathcal{F}_{bc}^*$, i.e. $\hat{\mathcal{U}}_{bc}^\top$, with the boundary coefficients of $\delta\mathcal{F}_{bc}$ in equation Eq. (A.17), two extra zeros need to be added to the end of vector $\hat{\mathcal{U}}_{bc}^\top$.

The double integral expressions in equations (A.4), (A.17), (A.24) and (A.34) combine to form the governing field equations (67), whereas the line integrals combine to form the governing boundary conditions (68). These equations feature two column vectors $\mathcal{L}_{eq}$ and $\mathcal{L}_{bc}$ that include the Lagrange multipliers $(u_{x_0}, u_{y_0}, w_0)$ and $(u_{n_0}, u_{s_0}, w_0)$, respectively, and their derivatives. These column vectors are derived from the Lagrange multiplier terms in Eq. (A.24), and are given by

$$\mathcal{L}_{eq} = \begin{bmatrix} -\left( \boldsymbol{D} \begin{Bmatrix} u_{x_0} \\ u_{y_0} \end{Bmatrix} \right)^\top & \nabla^\top \boldsymbol{D}^\top w_0 & 0 & \dots \end{bmatrix}^\top = -\begin{bmatrix} \epsilon_0^\top & \kappa^\top & \mathbf{0} \end{bmatrix}^\top \quad \text{(A.35)}$$

where

$$\epsilon_0^\top = \begin{bmatrix} \frac{\partial u_{x_0}}{\partial x} & \frac{\partial u_{y_0}}{\partial y} & \frac{\partial u_{x_0}}{\partial y} + \frac{\partial u_{y_0}}{\partial x} \end{bmatrix}$$

$$\kappa^\top = \begin{bmatrix} -\frac{\partial^2 w_0}{\partial x^2} & -\frac{\partial^2 w_0}{\partial y^2} & -2\frac{\partial^2 w_0}{\partial x \partial y} \end{bmatrix},$$

and

$$\mathcal{L}_{bc} = \begin{bmatrix} u_{n_0} & u_{s_0} & -(\nabla_{ns} w_0)^\top & 0 & \dots \end{bmatrix}^\top = \begin{bmatrix} u_{n_0} & u_{s_0} & -\frac{\partial w_0}{\partial n} & -\frac{\partial w_0}{\partial s} & 0 & \dots \end{bmatrix}^\top. \quad \text{(A.36)}$$

## References


[1] PA Hooper, RAM Sukhram, BRK Blackman, and JP Dear. On the blast resistance of laminated glass. *International Journal of Solids and Structures*, 49:899–918, 2012.

[2] PC Ciarlet, L Trabucho, and JM Viano. *Asymptotic Methods for Elastic Structures.* Walter de Gruyter & Co, 1995.

[3] W Yu, VV Volovoi, DH Hodges, and X Hong. Validation of the variational asymptotic beam sectional analysis (VABS). *AIAA Journal*, 40(10):2105–2113, 2002.

[4] G Kirchhoff. Uber das Gleichgewicht und die Bewegung einer elastischen Scheibe. *Journal fur reine und angewandte Mathematik*, 40:51–88, 1850.

[5] AEH Love. *The Mathematical Theory of Elasticity*. Cambridge University Press, London, 1934.

[6] RM Jones. *Mechanics of Composite Materials*. Taylor & Francis Ltd, London, UK, 2nd edition, 1998.

[7] L Demasi. Partially zig-zag advanced higher order shear deformation theories based on the generalized unified formulation. *Composite Structures*, 94(2):363–375, 2012.

[8] E Carrera. Theories and finite elements for multilayered, anisotropic, composite plates and shells. *Archives of Computational Methods in Engineering*, 9(2):87–140, 2002.

[9] E Carrera. Theories and finite elements for multilayered plates and shells: A unified compact formulation with numerical assessment and benchmarking. *Archives of Computational Methods in Engineering*, 10(3):5216–5296, 2003.

[10] RD Mindlin. Influence of rotary inertia and shear on flexural motion of isotropic elastic plates. *Journal of Applied Mechanics*, 18:31–38, 1951.

[11] PC Yang, CH Norris, and Y Stavsky. Elastic wave propagation in heterogeneous plates. *International Journal of Solids and Structures*, 2:665–684, 1966.

[12] M Levinson. A new rectangular beam theory. *Journal of Sound and Vibration*, 74(1):81–87, 1981.

[13] JN Reddy. A refined nonlinear theory of plates with transverse shear deformation. *International Journal of Solids and Structures*, 20(9):881–896, 1983.

[14] FB Hildebrand, E Reissner, and GB Thomas. Notes on the foundations of the theory of small displacements of orthotropic shells. Technical Note 1833, National Advisory Committee for Aeronautics, 1938.

[15] KH Lo, RM Christensen, and EM Wu. A high-order theory of plate deformation - Part 2: Laminated plates. *Journal of Applied Mechanics*, 44(4):669–676, 1977.

[16] RMJ Groh and PM Weaver. Static inconsistencies in certain axiomatic higher-order shear deformation theories for beams, plates and shells. *Composite Structures*, 120:231–245, 2015.

[17] E Carrera and G Giunta. Refined beam theories based on Carrera's unified formulation. *International Journal of Applied Mechanics*, 2(1):117–143, 2010.

[18] E Carrera and M Petrolo. Refined one-dimensional formulations for laminated structure analysis. *AIAA Journal*, 50(1):176–189, 2012.

[19] L Demasi. $\infty^3$ hierarchy plate theories for thick and thin composite plates: The generalized unified formulation. *Composite Structures*, 84:256–270, 2008.

[20] E Carrera. Developments, ideas and evaluations based upon Reissner's mixed variational theorem in the modeling of multilayered plates and shells. *Applied Mechanics Reviews*, 54(4):301–329, 2001.

[21] JM Whitney. Stress analysis of thick laminated composite and sandwich plates. *Journal of Composite Materials*, 6(4):426–440, 1972.

[22] A Tessler and HR Riggs. Accurate interlaminar stress recovery from Finite Element Analysis. Technical Memorandum 109149, NASA, 1994.

[23] R Rolfes and K Rohwer. Improved transverse shear stresses in composite finite elements based on first order shear deformation theory. *International Journal for Numerical Methods in Engineering*, 40:51–60, 1997.

[24] R Rolfes, K Rohwer, and M Ballerstaedt. Efficient linear transverse normal stress analysis of layered composite plates. *Computers & Structures*, 68(6):643–652, 1998.

[25] G Kuhlmann and R Rolfes. A hierarchic 3D finite element for laminated composites. *International Journal for Numerical Methods in Engineering*, 61:96–116, 2004.

[26] E Reissner. On the theory of bending of elastic plates. *Journal of Mathematics and Physics*, 23:184–191, 1944.

[27] E Reissner. The effect of transverse shear deformation on the bending of elastic plates. *Journal of Applied Mechanics*, 12(30):A69–A77, 1945.

[28] RC Batra and S Vidoli. Higher-order piezoelectric plate theory derived from a three-dimensional variational principle. *AIAA Journal*, 40(1):91–104, 2002.

[29] RC Batra, S Vidoli, and F Vestroni. Plane wave solutions and modal analysis in higher order shear and normal deformable plate theories. *Journal of Sound and Vibration*, 257(1):63–88, 2002.

[30] E Cosentino and PM Weaver. An enhanced single-layer variational formulation for the effect of transverse shear on laminated orthotropic plates. *European Journal of Mechanics A/Solids*, 29:567–590, 2010.

[31] RMJ Groh and PM Weaver. On displacement-based and mixed-variational equivalent single layer theories for modelling highly heterogeneous laminated beams. *International Journal of Solids and Structures*, 59:147–170, 2015.

[32] F Auricchio and E Sacco. Refined first-order shear deformation theory models for composite laminates. *Journal of Applied Mechanics*, 70(3):381–390, 2003.

[33] E Reissner. On a certain mixed variational theorem and a proposed application. *International Journal for Numerical Methods in Engineering*, 20(7):1366–1368, 1984.

[34] H Murakami. Laminated composite plate theory with improved in-plane responses. *Journal of Applied Mechanics*, 53:661–666, 1986.

[35] M Gherlone. On the use of zigzag functions in equivalent single layer theories for laminated composite and sandwich beams: A comparative study and some observations on external weak layers. *Journal of Applied Mechanics*, 80:1–19, 2013.

[36] A Tessler, M Di Sciuva, and M Gherlone. Refinement of Timoshenko beam theory for composite and sandwich beams using zigzag kinematics. Technical Publication 215086, National Aeronautics and Space Administration, 2007.

[37] A Tessler, M Di Sciuva, and M Gherlone. Refined zigzag theory for laminated composite and sandwich plates. Technical Publication 215561, National Aeronautics and Space Administration, 2009.

[38] A Tessler, M Di Sciuva, and M Gherlone. Refined zigzag theory for homogeneous, laminated composite, and sandwich plates: A homogeneous limit methodology for zigzag function selection. Technical Publication 216214, National Aeronautics and Space Administration, 2010.

[39] A Tessler, M Di Sciuva, and M Gherlone. A consistent refinement of first-order shear deformation theory for laminated composite and sandwich plates using improved zigzag kinematics. *Journal of Mechanics of Materials and Structures*, 5(2):341–367, 2010.

[40] RMJ Groh, PM Weaver, and A Tessler. Application of the Refined Zigzag Theory to the modeling of delaminations in laminated composites. Technical Memorandum NASA/TM-2015-218808, NASA, 2015.

[41] A Tessler. Refined zigzag theory for homogeneous, laminated composite, and sandwich beams derived from Reissner's mixed variational principle. *Meccanica*, Advances In The Mechanics Of Composite And Sandwich Structures:1–26, 2015.

[42] L Iurlaro, M Gherlone, M Di Sciuva, and A Tessler. Refined zigzag theory for laminated composite and sandwich plates derived from Reissner's mixed-variational theorem. *Composite Structures*, 133:809–817, 2015.

[43] M Di Sciuva, M Gherlone, L Iurlaro, and A Tessler. A class of higher-order C0 composite and sandwich beam elements based on the refined zigzag theory. *Composite Structures*, 132:784–803, 2015.

[44] MW Hyer and HH Lee. The use of curvilinear fiber format to improve buckling resistance of composite plates with central circular holes. *Composite Structures*, 18:239–261, 1991.

[45] Z Gurdal and R Olmedo. In-plane response of laminates with spatially varying fiber orientations: Variable stiffness concept. *AIAA Journal*, 31(4):751–758, 1993.

[46] PM Weaver, KD Potter, K Hazra, MAR Saverymuthapulle, and MT Hawthorne. Buckling of variable angle tow plates: From concept to experiment. In *Proceedings of the 50th AIAA/ASME/ASCE/AHS/ASC Structures, Structural Dynamics, and Materials Conference*, Palm Springs, USA, 2009.